1   REVISION 1

2

3

4   Glass structure, melt structure and dynamics: some concepts for petrology

5   Jonathan F. Stebbins*

6   Department of Geological Sciences

7   Stanford University, Stanford CA 94305, USA

8

9

10

11

12

13

14

15

16

17

18

19   _____

20   *corresponding author, stebbins@stanford.edu

21

1

Abstract

22

23   The thermodynamic and transport properties of the aluminosilicate melts at the heart of

24   most magmatic processes vary in complex ways with composition, temperature and pressure.

25   Insights into these properties can come from information on the structure of the melts

26   themselves, and more commonly from their glassy, quenched equivalents. Although most such

27   connections remain qualitative or semi-quantitative, they are fundamentally important in

28   interpretation of observations on igneous systems in nature and the laboratory, and in the

29   formulation of physically accurate models. This review presents some of the important concepts

30   of aluminosilicate glass and melt structure and dynamics that are most relevant to furthering our

31   understanding of the igneous processes so central to how our planet has formed and evolved. The

32   relationships among glasses, melts and crystals are introduced. The structural underpinnings of

33   temperature and pressure effects on melt free energies, densities and viscosities, constraints on

34   the extent of order/disorder among cations and anions in melts, why silica activity varies so

35   strongly with composition, and how liquid-liquid phase separation can be understood, are

36   discussed. Some simple, but useful, general views are presented on melt disorder and the shapes

37   of liquidus surfaces (key to magmatic phase equilibria), as are links between atomic-scale

38   dynamics and viscous flow and diffusion.

39   **Keywords:** silicate melt, glass structure, phase equilibria, viscosity, igneous process

40

Introduction

41

42   After decades of research using many experimental and theoretical approaches, much is

43   now known about the structure of aluminosilicate glasses. These materials are of interest not

44   only to igneous processes in nature, but in advanced technologies as well. Less well defined are

2

45   the high temperature (and often high pressure) liquids themselves, but work on glasses has

46   provided a basic framework, and growing numbers of in-situ, high T, high P, and even high P/T

47   experiments are becoming feasible. However, as may be inevitable in a developing field, the

48   specialized language and concepts of the discussion, and the focus on ever-finer quantitative

49   details, can limit accessibility by non-experts. This can, in turn, limit motivating inputs from

50   those studying petrological processes into future directions of investigations on the atomic-scale.

51   Conversely, phenomenological models that are generated to make pragmatic predictions of melt

52   properties, such as compositional fits of phase equilibria or physical property data, may have

53   limited physical accuracy if they are not well-informed by structural concepts. And, a more

54   general understanding, by a wider scientific community, of the fundamental roots of well-known

55   petrological phenomena may lead to new insights into how igneous processes occur in nature as

56   well as the laboratory or industrial glass production facility. Increasingly accurate, and more

57   automated, tools have been developed for calculating the behavior of melts, which often now

58   appear as "black box" software packages. The very success of such modeling efforts can

59   actually insulate users from underlying connections between structure, atomic-scale process, and

60   melt properties, obscuring fundamental and intriguing questions. For example, *why* do the heats

61   and entropies of fusion for minerals, buried in a model algorithm, vary so greatly, and *why* does

62   this matter so much for geological systems?

63   It is thus the purpose of this review to present some of the basic concepts of melt

64   structure and properties in a brief, non-technical form that may increase their accessibility to

65   students and researchers of real-world igneous processes, and enhance the two-way cross-

66   fertilization that can enhance progress across the entire spectrum. Given the breadth of this field,

67   and the limitations of a relatively short article, not much detail can be provided. Recent

3

68 introductions to the field (Calas et al., 2006; Dingwell, 2006; Galoisy, 2006; Henderson et al.,

69 2006), as well as more extensive reviews, provide not only greater conceptual depth but the

70 background literature from experiment and theory that lies beneath the generalizations given here

71 (Greaves and Sen, 2007; Lee et al., 2004; Mysen, 1990; Mysen and Richet, 2005; Richet and

72 Bottinga, 1986; Richet and Neuville, 1992; Stebbins et al., 1995a; Stebbins et al., 2013; Stebbins

73 and Xue, 2014). Several areas of particular interest in petrology, where some real progress has

74 been made in connecting melt structure with macroscopic properties, are also neglected here for

75 length reasons, notably the role of volatile components such as H_2O, and crystal-melt

76 partitioning. Insights from quantum chemical calculations and computer simulations, which have

77 long been important in thinking about melt structure and properties (deJong and Brown, 1980;

78 Navrotsky et al., 1985; Tossell and Vaughn, 1992) and which are increasingly being extended to

79 large-scale Earth processes (Ghosh et al., 2014; Richet and Ottonello, 2014; Stixrude et al.,

80 2009), also largely fall outside the scope of this article.

81

82 **Crystals vs. liquids vs. glasses**

83 *Melting, crystallization, and the glass transition*

84   The processes of melting and crystallization are of course of key importance in igneous

85 systems, and are ultimately controlled in part by the atomic-scale structure of the melt. However,

86 these are not the main subjects of this review. On the other hand, quenching of silicate melts to

87 glasses does happen to be a common phenomenon in nature, especially during rapid cooling of

88 magmas on the sea floor and in explosive eruptions. More generally, much of what we know

89 about the atomic-scale structure of silicate melts comes from diffraction and spectroscopic

4

90   studies of glasses. It is thus important to know just what a glass is, what it is not, and what it

91   represents.

92   When a crystalline solid melts to a liquid, there are abrupt changes in first order

93   thermodynamic properties including enthalpy, entropy and volume, as well as their "second

94   order" temperature and pressure derivatives, namely constant pressure heat capacity (C_P),

95   thermal expansivity ($\alpha = [dV/dT]/V$), and compressibility ($\beta = -[dV/dP]/V$). Under equilibrium

96   conditions, melting occurs as heat energy (enthalpy) is added to break bonds and rearrange and

97   (usually!) expand the structure, with an entropy increase to balance the free energy change to

98   zero. The crystal, defined by long range as well as at least partial short range order, transforms

99   from a relatively rigid state to a more fluid, more disordered state in which ions or molecules are

100   much more mobile.

101   Going the opposite direction, the kinetics of crystal nucleation and growth can be

102   relatively slow. Especially in liquids where the viscosity at the melting point (T_m, or the liquidus

103   temperature) is relatively high, as is often the case for silicate melts, the temperature can be

104   lowered below T_m without crystallization taking place, into the metastable, "supercooled" liquid

105   region. High viscosity is closely associated not only with slow diffusion of the components that

106   need to assemble to make a complex crystal from the liquid, but also with the short-range bond

107   breaking and re-arrangements that are needed to go from the disordered melt structure to what

108   may be a quite different structure in the crystal. With falling temperature, all of these dynamics

109   slow down as the viscosity rises; if cooling is sufficiently rapid, crystallization may be avoided

110   completely. With cooling, the structure of the liquid itself continuously re-arranges and becomes

111   more ordered as its entropy decreases. At some point, however, the kinetics of the local structural

112   changes needed to maintain metastable equilibrium in the melt become too slow to keep pace

5

113   with the decreasing temperature. Over a temperature interval that is typically only a few to 10's

114   of degrees, the liquid falls out of equilibrium and the melt structure "freezes in" to form a rigid

115   glass. At typical laboratory cooling rates this occurs at a viscosity of about 10^{12} Pa·s, whether the

116   liquid is a geologically interesting basalt, a multi-component borosilicate in a production line

117   making glass for computer displays, or a simple organic molecular liquid such as glycerol.

118   The transition from liquid to glass involves often a large decrease in second order

119   properties– heat capacity, thermal expansivity and compressibility– over a fairly narrow

120   temperature interval, without abrupt changes in first order properties. It thus in some ways can

121   resemble a second order phase transition in a crystal. However, the glass transition is inherently a

122   kinetic phenomenon depending on thermal history and structural dynamics, and is thus a

123   disequilibrium process. Glasses *do* have physical properties that clearly define them as solids,

124   not just as "really viscous liquids", but they lack the long-range translational symmetry and order

125   of crystals.

126

127   *Fictive and glass transition temperatures*

128   A measure of where a liquid transforms to a glass during cooling is the "fictive

129   temperature" (T_f), which approximates the point where the melt structure was "frozen into" that

130   of the glass (Mysen and Richet, 2005). T_f will be higher if cooling is more rapid (Fig. 1);

131   correspondingly, the liquid will behave rigidly (and potentially fracture) at a higher temperature

132   and lower viscosity if deformation is very rapid (Dingwell and Webb, 1990). Obtainable

133   laboratory cooling rate variations over 6 or 8 orders of magnitude typically can change T_f by

134   only up to about 200 ˚C, however. This means that some structural details important in liquids at

135   much higher temperatures are potentially not detectable in any glass that can be formed and must

6

136   be observed in situ or in computer simulations. The closely related term "glass transition

137   temperature" (T_g) is often used in a similar sense to T_f, but most commonly designates the point

138   at which a glass, heated at a standard rate such as 10 ˚C/minute, transforms back to a metastable

139   supercooled liquid with a measurable change in C_p or α. It is very important to note that the melt

140   structure recorded in the glass should depend only on the cooling rate through the glass transition

141   range and *not* on the initial temperature, assuming that the original stable liquid is truly a single

142   phase (no residual crystals or bubbles) and that cooling is isochemical. In some systems the latter

143   may not be the case, as temperature can drive compositional changes, most obviously variations

144   in oxidation state of Fe and other redox-variable elements. Because such kinetics may involve

145   longer-range diffusion of chemical components, their structural consequences may occur much

146   more slowly than the processes that control local isochemical structure and viscosity.

147   A glass with a faster cooling rate and higher T_f will thus have a greater enthalpy of

148   formation and a greater molar volume (lower density) than the same composition glass with a

149   lower T_f, differences that can often be readily measured in the lab on experimental (Tischer,

150   1969) and sometimes on natural glassy materials (Dingwell, 2006; Nichols et al., 2009). A glass

151   with higher T_f will also inherit a higher degree of structural disorder from the metastable liquid.

152

153   *Configurational properties of melts-why structure matters*

154   Thermodynamic properties, most obviously free energy and its first (entropy, volume)

155   and second temperature and pressure derivatives (involving C_p, α, β), control melting and

156   crystallization and thus define the phase diagrams at the heart of igneous processes. Melt

157   properties, and how they change with composition, are closely linked to melt structure. While it

158   is not yet possible to accurately predict the details of phase equilibria from structural

7

159   measurements alone, knowledge of these connections is critical to testing and improving models

160   as well as fundamental in understanding the atomistic roots of complex geological processes.

161   The heat capacity of both crystalline and glassy solids is usually dominated by the energy

162   put into interatomic vibrations with increasing temperature, and increases with temperature. For

163   materials such as silicates that have relatively high melting and glass transition temperatures, it

164   has long been observed that the heat capacity (most precisely the constant volume heat capacity

165   C_V, which for solids usually differs from C_P by only a few %) tends to approach the classical

166   vibrational limit of about 3 times the gas constant R per mole of atoms (Mysen and Richet, 2005;

167   Richet, 1984). Heat capacities well above this value may be observed when extra energy needs to

168   be added to change the structure itself with increasing temperature. This involves rearranging the

169   atoms or molecules and the bonds between them, and associated increases in C_P are often thus

170   considered as "configurational" ($C_{P,conf}$). Such effects can be observed in some crystalline phase

171   transitions involving cation or anion disorder, and in crystalline molecular solids in which whole

172   molecules can begin to rotate or exchange positions. $C_{P,conf}$ for silicate melts is sometimes

173   approximated simply as the excess over 3R per mole of atoms, or more commonly as the

174   increment in C_P between glass and liquid at T_g, which is usually similar. In most melts more

175   complex than SiO_2 itself, such configurational heat capacities are quite significant (10 to as much

176   as 50% above the 3R "limit"), are readily observed on heating through T_g, and, when integrated

177   up in temperature to melting points, have large effects on overall entropy, enthalpy and free

178   energy. For example, the heat of fusion of diopside ($CaMgSi_2O_6$) at its melting point would be

179   estimated as about 86 kJ/mol if the configurational component of C_P were neglected, that is, if

180   the liquid heat capacity were taken as that of the glass; the actual value is about 138 kJ/mole

181   (Richet and Bottinga, 1986). Increases in thermal expansivity and compressibility are usually

8

182   even larger than those in C_P, often growing by a factor of two or three from glass to liquid

183   (Mysen and Richet, 2005; Richet and Neuville, 1992). If these property changes are

184   "configurational", the obvious and fundamental questions are "what is the structure?" and "how

185   is it changing so much with temperature?"

186   As a preview to structural concepts discussed below, it's useful to compare the properties

187   of albite liquid ($NaAlSi_3O_8$) with those of a lower silica composition such as diopside

188   ($CaMgSi_2O_6$). As a rough starting point, the former may be considered to represent something

189   resembling a high-silica rhyolite, the latter a mafic, even ultramafic magma. The structures of the

190   feldspar and pyroxene crystals are of course very different, and it is safe to assume that the melt

191   structures will also be very different. The enthalpies and entropies of melting, per mole of atoms,

192   are also very different: ΔH_m and ΔS_m for diopside are 13.8 kJ/mole of atoms (138 kJ/mole

193   divided by10 atoms per formula unit) and 8.3 J/K/mole of atoms, but for albite are 4.9 kJ/mole of

194   atoms and 3.5 J/K/mole of atoms. Increases in heat capacity on heating through T_g are also quite

195   different, about 31 % vs. 8% for diopside and albite liquids respectively (Richet and Bottinga,

196   1986).

197   Beyond the obvious importance of configurational (structural) changes and consequent

198   effects on thermodynamic properties to phase equilibria, heat budgets, melt density and

199   buoyancy, etc., there is a remarkable and fundamental connection between *transport* properties

200   of melts, most obviously viscosity, and the configurational heat capacity and entropy. As noted

201   above, for typical cooling rates the viscosity of almost any glass forming liquid is about 10^{12} Pa.s

202   at its transition to glass, including for example, a rhyolite and a basalt, or albite and diopside as

203   illustrated here; and T_g's for all of these typically differ by only about 100 K. However, the rate

204   at which viscosity (η) decreases with T above T_g, and the shape of the curve on a plot of log η

9

205   vs. inverse 1/T (an "Arrhenius" plot) differ greatly (Fig. 2). Liquids such as silica, albite, and

206   anhydrous rhyolites have such curves that are nearly linear ("Arrhenian" behavior) over as much

207   as 1000 K, and have been labeled as "strong" liquids (Angell, 1985). The configurational

208   components of their heat capacities are relatively small, suggesting that structural change with T

209   is limited. In contrast, η for a composition such as diopside or a mafic basalt decreases much

210   more rapidly above T_g, then curves to a shallower slope at high T, resulting in a viscosity in the

211   magmatic temperature range that may be many orders of magnitude below that of a "strong"

212   liquid. (Of course, basaltic magmas in nature are generally much hotter than rhyolitic magmas,

213   which accentuates their difference in viscosities). Such liquids are described as more "fragile".

214   Their systematically higher increases in C_P at T_g suggest more rapid structural disordering with

215   rising temperature. Models that parameterize viscosity as functions of composition, regardless of

216   their theoretical basis, must include this sometimes highly "non-Arrhenian" temperature

217   dependence to be accurate and useful over a wide temperature range (Giordano et al., 2006; Hess

218   et al., 1996; Mauro et al., 2009).

219   These fundamental relations, which apply to many types of glass formers from simple

220   organic molecular liquids and polymers, molten salts, and even some aqueous solutions, as well

221   to more conventional silicate-based systems, were highlighted by physicists and chemists

222   working on the intriguing general issue of the nature of the glass transition (Angell, 1985). The

223   "Adam-Gibbs" equation (Mysen and Richet, 2005; Richet, 1984) draws the quantitative

224   connections:

225         $$\log \eta \ = A \ + \ B/ (T \, \Delta S_{conf}) \qquad\qquad\qquad\qquad (1)$$

226   where S_{conf} is the configurational entropy of the liquid, based on the value at T_g and integration

227   up in temperature of its derivative, $C_{P,conf}/T$, from T_g. A and B are fitting parameters needed to

10

228   match the shape of the viscosity curve, but may be correlated with each other in a given type of

229   material. The applicability of the Adam-Gibbs equation to silicate melts of interest in the

230   geoscience community has been well-demonstrated by calorimetry and viscosity studies in both

231   pioneering early studies (Richet, 1984) and recent re-confirmations (Richet, 2009); it has often

232   been inverted to estimate configurational entropies from viscosity data on complex silicate melt

233   solutions and test models of mixing (Neuville and Richet, 1991; Toplis et al., 1997a). The exact

234   physical explanation of the Adam-Gibbs equation in such liquids remains incompletely

235   understood, but it again points out how fundamental the liquid structure, and how it changes with

236   temperature, must be to the melt properties that control igneous processes.

237

238   **Concepts of melt structure-ties to magma properties**

239   The known structures of crystalline silicates, familiar ground for most Earth scientists,

240   provide the basic starting point for concepts of glass and melt structure, but can only take us so

241   far into the disordered, dynamical realm of high temperature liquids. The literature of glass

242   structure is vast because of widespread interest not only in the geosciences but in technology,

243   condensed matter physics, and solid-state chemistry. Here I will highlight a few basic concepts

244   that have some obvious bearing on petrologic processes.

245

246   *The silica network and network modifying oxides*

247   The common beginning for such discussions is pure silica (SiO_2). Glasses of this

248   composition are quite important in technology in optical components and data transmission

249   fibers, but are found in nature only in fulgurites and rare types of impactites (e.g. Libyan Desert

250   glass). As in the low-pressure crystalline forms of silica, it's well known that the glass is

11

251   comprised of a 3-dimensionally linked, corner-shared network of SiO_4 tetrahedra, with some

252   degree of disorder in the ring structure, bond angles, and distances. The oxygen links between

253   the Si^{4+} "network forming" cations are denoted "bridging" oxygens (BO). Si-O bonds in such

254   tetrahedra are among the strongest in silicate materials. Silica liquid thus is the epitome of a

255   "strong" liquid in the sense that its viscosity drops relatively slowly on heating above T_g, and its

256   heat capacity increase from glass to metastable liquid at T_g is minimal. It is thus not surprising

257   that cristobalite, the crystalline polymorph stable at the 1 bar melting point, has the lowest

258   known heat and entropy of fusion of any silicate (3.0 kJ/mole of atoms, 1.5 J/K/mole of atoms)

259   (Richet and Bottinga, 1986). This simple fact has a huge impact on silicate phase equilibria and

260   on magmatic differentiation, as will be discussed below. A 2-dimensional "cartoon" view of the

261   relatively minor structural differences between crystalline and glassy silica is shown in Figure 3.

262   When an oxide of another element with +1 or +2 valence (M_2O or MO, such as an alkali

263   or alkaline earth oxide) is added to liquid silica, there are too many oxygen anions (O^{2-}) for them

264   to all connect to two, tetrahedrally coordinated Si^{4+} cations. As a result, some must be bonded to

265   only one SiO_4 group and thus become "non-bridging" oxygens (NBO). In standard models,

266   which are good first approximations, exactly 2 NBO are formed from one BO and one added O^{2-}

267   ion (Fig. 4a):

268   Si-O-Si + M_2O ⇔ 2 Si–O^- + 2 M^+ (2)
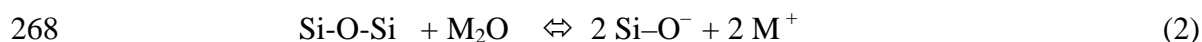
269   When enough modifier oxide has been added so that the molar ratio O/Si is greater than the

270   coordination number of Si (4), then there must be O^{2-} ions that are bonded only to the modifier

271   cations, forming so-called "free" oxide ions. Magmas this poor in silica (<33.3 mole %, as in

272   olivine) are rare in nature, but are of major importance in the technology of ore smelting, where

273   the properties of molten "slags" are key to the controlled reduction and purification of molten

12

274   metals such as iron. This species can also be present in minor amounts at higher silica contents,

275   at least when the "modifier" cation has a relatively high charge and/or small radius (e.g. Mg^{2+})

276   (Nasikas et al., 2012; Sen and Tangeman, 2008), tends to form relatively covalent bonds (e.g.

277   Pb^{2+}) (Lee and Kim, 2014)), or is part of an OH^- group bonded only to modifier cations (Xue,

278   2009).

279   Locally, the negative charge on each NBO (formally –1) must be balanced by

280   coordination with *several* modifier cations, each of which is shared, in turn, with other oxygens,

281   just as in crystalline silicates. And, of course, the energetically stable coordination number of the

282   modifier cation is generally much greater than the 1 or 2 NBO produced per cation by reaction

283   (2). Therefore, also as in crystals, at silica contents above the olivine composition, there are

284   usually not enough NBO to make up the full first-shell coordination of each modifier cation,

285   which thus must then include some BO. Many of the differences between effects of different

286   cations are captured by the variable "cation field strength", which is the valence divided by the

287   sum of the cation and oxide ion radii (e.g. $Mg^{2+} > Ca^{2+} > Na^+ > K^+$) (Brown et al., 1995). If

288   multiple types of modifier cations (M) are present in the melt, they may "compete" for the

289   formation of small coordination shells with short M-NBO distances, with the higher field

290   strength cation expected to "win", again as can be seen in some crystal structures. For example,

291   Ca^{2+} in crystalline diopside has 4 NBO and 4 BO neighbors, while smaller Mg^{2+} has 6 neighbors,

292   all NBO. Modifier cations will thus interact with not only the NBO in their first shells, but with

293   any BO present as well. In liquids these interactions are dynamic, transient, and likely to be

294   important in breaking BO-Si bonds, which is required for viscous flow to occur in all but the

295   most silica-poor melts. Mixing of different modifier cations, if it occurs, will add to

296   configurational entropy of the melt, affecting its viscosity curve and fundamental

13

297   thermodynamics. For example, unlike in the crystal, there is evidence of a randomized Ca/Mg

298   distribution in diopside glass and liquid, with a large contribution of this mixing to the entropy of

299   fusion (Allwardt and Stebbins, 2004; Cormier and Cuello, 2013; Richet and Bottinga, 1986;

300   Stebbins et al., 1984). Another 2-D "cartoon" view of the wide range of possibilities for

301   structural disorder in a complex, lower silica composition such as multi-component chain silicate

302   is shown in Figure 5. As in crystals, most modifier cations can themselves have a range of

303   coordination numbers in melts and glasses, which can vary in complex ways with composition,

304   temperature, and pressure (Brown et al., 1995; Farges et al., 1994; Farges et al., 1996; Galoisy,

305   2006; Guignard and Cormier, 2008; Skinner et al., 2012; Wilke et al., 2007).

306

307   *Composition, structure and "fragility" in simple binary systems*

308   It is not really the modifier *cations* that "break up" the silica network (as is often stated in

309   introductions to this topic), but the accommodation of the added oxide ions into the network,

310   which must reduce the number of bridges between the Si cations if the latter remain coordinated

311   by exactly 4 oxygens. However, modifier cation-BO interactions *do* weaken the silicate network

312   by pulling some electron density out of the Si–O–Si linkages, and bonds among the modifier

313   cations and the NBO are generally more ionic, weaker, and longer than Si–O bonds. The liquid

314   thus becomes more "fragile" as more modifier oxide is added, and viscosity at $T > T_g$ drops

315   farther and farther below that of liquid silica. Heat capacity increase at T_g becomes larger and

316   larger as well, and the liquid structure becomes disordered more and more rapidly with

317   increasing temperature. As noted above, heats and entropies of fusion tend to increase with

318   decreasing silica content, at least in part because of the greater number of ways that a low-silica

14

319   melt can be disordered. Some aspects of these changes in disorder are known, many are still to

320   be determined.

321

322   *Clustering and liquid-liquid phase separation*

323   The size and charge of the modifier cation systematically affect the quantitative details of

324   property changes with composition. For example, modifier cations usually are energetically

325   stabilized more effectively by NBO than by BO. This can lead to preferential clustering of NBO

326   with these cations, and eventually to liquid-liquid phase separation. Two-liquid fields extend

327   systematically to higher temperatures and wider ranges of silica contents with higher modifier

328   cation field strength. One of the highest field strength modifiers that is abundant in magmas, and

329   that is often concentrated during differentiation under low f_{O2} conditions, is FeO. It is thus not

330   coincidental that the only common observation of silicate liquid-liquid phase separation in nature

331   is in very FeO-rich residual melts trapped in some crystallizing basalts. As will discussed below,

332   closely related effects of field strength and network species distributions have petrologically

333   critical effects on one of the most important chemical parameters, the thermodynamic activity of

334   silica. Some cation and NBO clustering may be common even in single-phase melts, leading to

335   the possibility of through-going "ion channels" (Greaves and Sen, 2007) that may greatly

336   augment diffusion in both liquids and glasses (Fig. 6)

337

338   *Melt structure vs. mineral structure*

339   In a general sense, the *continuous* change with composition in a "snapshot" view of melt

340   structure at high temperature, or in the quenched-in structure at the glass transition that can

341   actually be observed at room temperature, resembles the *discontinuous* progression in the

15

342   structures of crystals as the modifier oxide/silica ratio increases, and hence the ratio of NBO to

343   tetrahedral cations (NBO/T). In the Na_2O-SiO_2 system, for example, crystalline $Na_2Si_2O_5$

344   ($Na_2O/SiO_2 = 0.5$) is a sheet silicate analogous to a mica: the average NBO/T must be 1 (reaction

345   1). It happens that each SiO_4 group in the crystal actually has just one NBO and 3 BO, although

346   other distributions could be imagined in a more complex structure of the same composition. At

347   $Na_2O/SiO_2 = 1.0$ the chain silicate Na_2SiO_3 forms with each tetrahedron having exactly 2 NBO;

348   at $Na_2O/SiO_2 = 2.0$ an olivine-like structure Na_4SiO_4 is stable and each SiO_4 has 4 NBO and no

349   BO. In rock-forming minerals the progression from sheet silicates to pyroxenes to olivines

350   follows the same pattern, although compositions are often more complex. Spectroscopy (e.g.

351   Raman and NMR) on simple-composition glasses can detect and sometimes count SiO_4

352   tetrahedra with varying numbers of BO and NBO (Koroleva et al., 2013; Maekawa et al., 1991;

353   Malfait et al., 2007b; Mysen and Richet, 2005). In some early literature these were described as

354   "sheet-like", "chain-like" (etc.) units by analogy with the crystals. However, these terms may

355   inadvertently carry implications about longer range structure and dynamics for which we have

356   little real information. Hence, a terminology has been adopted that fixes the description to the

357   measureable local structure of SiO_4 groups ("Quaternary," with four bonds) with varying number

358   ($n = 0$ to 4) of bridging oxygens, "Q^n species". Low-pressure crystalline silica is thus solely

359   comprised of Q^4 units, pyroxenes of only Q^2 units, olivines of Q^0 and so forth. An obvious

360   question for melt and glass structure thus becomes how do distributions of Q^n species relate to

361   those known to be present in the crystals.

362

363   *Network speciation, modifier cations and silica activity*

16

364   One of the early hints about the nature of structural disorder in glasses, and of its

365   quantitative extent, relates to such network speciation, and is closely linked to one of the most

366   important thermodynamic parameters needed to understand and predict magmatic phase

367   equilibria, namely the activity of silica (a_{SiO2}). As introduced by slag chemists and as highlighted

368   for petrologists in the seminal work of I.S.E. Carmichael (Carmichael et al., 1974), silica activity

369   controls not only the solubility of silica minerals but equilibria between pairs of major rock-

370   forming silicate minerals such as feldspars-feldspathoids and pyroxenes-olivines. It is thus

371   fundamental to magmatic evolution and even to standard igneous rock classification schemes. It

372   has been known since early phase diagram studies (Hess, 1995; Ryerson, 1985) that modifier

373   cation field strength systematically and dramatically affects the activity coefficient of silica in

374   melts ($\gamma_{SiO2} = a_{SiO2}/X_{SiO2}$).

375   Figure 7 (Ryerson, 1985) shows the silica saturation curves (liquidi) for a series of

376   alkaline earth and alkali oxide-silica binaries. In each such binary phase diagram, isothermal

377   points on the cristobalite liquidus each must have the same silica activity. The mole fraction of

378   silica at such points steadily decreases as the field strength increases from K^+ to Na^+ to Li^+ to

379   Ba^{2+} to Sr^{2+} to Ca^{2+} to Mg^{2+} (see (Brown et al., 1995) for field strength values). The activity

380   coefficient γ_{SiO2} must thus increase, by a factor of almost 2, in this same sequence. Similar

381   systematics have also long been known in three-component phase equilibria where a_{SiO2} is fixed

382   by mineral pairs such as forsterite-enstatite (Hess, 1995; Ryerson, 1985).

383   This systematic effect continues into complex multicomponent magmatic liquids, as can

384   be explored by calculation of a_{SiO2} using the pMELTS software package (Ghiorso et al., 2002), in

385   the composition, temperature and pressure range where it is well-calibrated, such as for basaltic

386   melts at 1600 ˚C and 1 GPa. For a standard MORB composition (51 mole % SiO_2), 1 mol %

17

387   CaO can be systematically replaced with 1 mol % of K_2O, Na_2O, MgO, or FeO (Fig. 8). Here,

388   the same qualitative trend as expressed in the simple binary and ternary systems is readily

389   apparent, with a steady increase in a_{SiO2} with smaller and/or higher charged modifier cations. In

390   an extreme example of replacing 6% MgO in a typical MORB with Na_2O, the average modifier

391   cation field decreases from 0.39 to 0.32 and γ_{SiO2} drops by a factor of 2.5; a typical K and Na-

392   rich, Ca- and Mg-poor nephelinite (average cation field strength of 0.34, 41 mole % SiO_2) has

393   γ_{SiO2} about 4 times lower than the unmodified, low-alkali, high Mg MORB.

394   This dramatic effect is well, if qualitatively, correlated with findings on glass and melt

395   structure. A melt of the same composition as a simple binary silicate crystal, such as $Na_2Si_2O_5$ or

396    $MgSiO_3$, could be imagined to have exactly the same Q^n speciation as the crystal, i.e. all Q^3 or all

397   Q^2 in these examples. Spectroscopy on glasses and melts has shown instead that

398   "disproportionation" reactions take place, probably driven by the entropy generated by mixing of

399   a greater variety of Q^n species than is necessitated by composition alone, such as:

400          $2Q^3 \Leftrightarrow Q^4 + Q^2$ (3)

401          $2Q^2 \Leftrightarrow Q^3 + Q^1$ (4)

402   The right hand sides of such reactions are generally favored by higher field strength modifier

403   cations (Davis et al., 2011; Maekawa et al., 1991; Malfait et al., 2007a; Mysen and Richet,

404   2005), as groups with lower Q^n numbers have more concentrated local negative charge (more

405   NBO in one place). As a "side effect", the concentration of Q^4 units is higher in such systems

406   (e.g. Li>Na>K), which correlates systematically with higher γ_{SiO2}. For example, in the alkali

407   disilicate glasses ($M_2Si_2O_5$), which *could* be comprised of only Q^3 units, about 17, 11, and 7 %

408   Q^4 species have been detected for Li vs. Na vs. K by ^{29}Si NMR spectroscopy (Maekawa et al.,

409   1991), balanced by corresponding concentrations of Q^2 and other groups. Quantitative

18

410 connections between such structural details and the phase diagrams have been made in models of

411 simple alkali silicate binaries (Gurman, 1990; Vedishcheva et al., 1998); extending them to

412 detailed structure-free energy links in complex magmatic systems remains for the future. The

413 mixing of Q^n species contributes significantly to the overall configurational entropy of the melt

414 but is by no means the predominant term. Reactions such as (3) and (4) generally seem to have

415 positive enthalpy changes and thus shift to the right at higher temperatures, but much remains to

416 be learned about such details even in simple systems.

417

418 *Aluminum, network order/disorder, and silica activity*

419 The Al^{3+} cation is only slightly larger than Si^{4+}, and thus at low pressures is largely four-

420 coordinated in aluminosilicate melts and glasses of geological compositions. If Al_2O_3 (or, more

421 clearly for comparison with SiO_2, $AlO_{3/2}$) is added to a binary modifier-silicate melt, there is a

422 per-cation deficit of oxygen relative to SiO_2. This means that to provide four oxygens to

423 coordinate the Al, NBO must be converted to BO (Fig. 9). Unlike the effectively charge-neutral

424 BO connecting two SiO_4 groups, those linking AlO_4 groups to other network-formers have a net

425 partial negative formal charge, –1/4 in the case of Al-O-Si and –1/2 in the case of Al-O-Al.

426 These charges are based on simple considerations of bond valence sums (Brown et al., 1995;

427 Brown and Shannon, 1973), e.g. Al^{3+} with four Al-O bonds contributes +3/4 to each O, an

428 adjacent Si^{4+} with four Si-O bonds contributes +4/4, and the difference between the O^{2-} valence

429 and 7/4 is –1/4. Actual electron distributions, for example as calculated by ab initio methods

430 (Vuilleumier et al., 2011), will be somewhat different and will vary with details such as bond

431 angles and distances, but the relative trends illustrated by such approximations have long been

432 shown to be useful starting points in thinking about both crystal and melt structure. Advanced

19

433   theoretical methods can, of course, be very useful in elucidating the fundamentals of cation-

434   oxygen interactions in this context (Gatti et al., 2012).

435   As AlO_4 tetrahedra become part of the strongly-bonded silicate network in glasses and

436   melts, the mixing of Al and Si, and of three instead of one distinct type of bridging oxygen, add

437   much complexity and many more options for the generation of configurational order/disorder

438   that is so important to bulk properties. Partial negative charges on Al-O-Si and Al-O-Al BO need

439   to be locally balanced, generally by the "modifier" cations, which in this role are often labeled as

440   "charge compensators". In the case of relatively large, low charge cations (e.g. K^+ or Na^+), it can

441   be difficult to fit enough neighbors to compensate the $-1/2$ charge on Al-O-Al: if the K^+ is eight

442   coordinated, for example, each cation will contribute only $+1/8$, in principle requiring 4 K^+

443   neighbors around an Al-O-Al bridging oxygen. This becomes difficult simply for local

444   volumetric reasons (sometimes called "steric hindrance" (Mysen and Richet, 2005)). The

445   consequence is what has long been known as "aluminum avoidance", meaning that Al-O-Al

446   linkages are minimized in favor of Si-O-Al plus Si-O-Si, which is possible if overall Al/Si <1 as

447   in all natural magmas. Equilibria such as that below are therefore shifted to the left:

448        $$2(\text{Si-O-Al})^{-1/4} \Leftrightarrow (\text{Si-O-Si})^{0} + (\text{Al-O-Al})^{-1/2} \tag{5}$$

449   The consequences of the ordering that can result have long been explored in the thermodynamics

450   of feldspars and other crystalline aluminosilicates (Putnis, 1992); "Al avoidance" is known to be

451   especially prevalent in alkali feldspars and feldspathoids, especially those formed at low

452   temperature where enthalpy is more likely to prevail over entropy. The presence of smaller,

453   higher charged "compensating" cations (e.g. Mg^{2+} or Ca^{2+} vs. Na^+ or K^+) can more readily

454   balance the charge on the Al-O-Al bridging oxygens, allowing such linkages to form in

455   disordered high temperature phases such as crystalline anorthite ($CaAl_2Si_2O_8$) near its melting

20

456   point (Phillips et al., 1992) and high temperature cordierite ($Mg_2Al_4Si_5O_{18}$) (Putnis et al., 1985).

457   In such materials the disordered structure is stabilized by the extra entropy of mixing of Al and

458   Si in the network. The same is certainly expected in melts. This has indeed been demonstrated by

459   spectroscopic studies of simple, ternary aluminosilicate glasses: some Al-O-Al can be observed

460   in Na aluminosilicates, but much less than in a fully random distribution of Al and Si;

461   comparable Ca aluminosilicates are more disordered (Lee and Stebbins, 2000; Stebbins et al.,

462   1999). Limited evidence from glasses prepared with different fictive temperatures shows the

463   expected increased randomness at higher T (Dubinsky and Stebbins, 2006). Network order-

464   disorder is schematically illustrated in Figure 10. Here, one sketch shows complete "avoidance"

465   of presumably energetically costly Al-Al pairs, the other a random distribution with a much

466   higher configurational entropy. In favorably cases, ^{17}O NMR and other methods can actually

467   count the distributions of the different oxygens (Al-O-Al, Al-O-Si, Si-O-Si) in glasses and

468   minerals, allowing development of thermodynamic models (Dirken et al., 1997; Lee and

469   Stebbins, 2000).

470   In melts with high Al/Si, such as $NaAlSiO_4$, the disorder generated by mixing of Si and

471   Al (and of the three kinds of BO) can be a substantial fraction of the overall configurational

472   entropy (Stebbins, 2008); in natural magmas with much lower Al/Si the effects are smaller.

473   However, because higher field strength modifiers push reactions such as (5) to the right, the

474   concentration of silica-like species, and thus of silica activity, is again enhanced. In more silica-

475   rich systems with few NBO and low probability of Al-O-Al, analogous re-distributions of Al and

476   Si neighbors around a given SiO_4 group probably also play a role (Murdoch et al., 1985). For

477   example, for silicate Q^4 groups connected to various numbers of AlO_4 groups (the rest being

478   SiO_4), an equilibrium can be written (one of many possible for different network species):

21

479 $\qquad 2Q^4[1Al] \iff Q^4[0Al] + Q^4[2Al]$ (6)
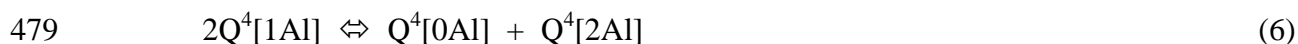
480 As for the right-most species in reactions (3) and (4) (i.e. lower Q^n numbers) and (5) (i.e. Al-O-

481 Al), the right-most species in reaction (6) has the highest local negative charge concentration,

482 and is stabilized by higher field strength modifier cations. All three reactions point to an

483 accompanying greater concentration of locally silica-like species, and thus higher γ_{SiO2}. This is

484 in fact again seen in analysis of simple pseudobinary phase diagrams such as $Ca_{0.5}AlO_2$-SiO_2 and

485 $NaAlO_2$-SiO_2 (Ryerson, 1985), where a shift in silica liquidus compositions analogous to those

486 in simple binary silicates has long been known.

487 $\qquad$ In summary, alkali-rich melts will have much lower silica activities than MgO-, CaO-, or

488 FeO- rich melts of the same molar proportions. The products of magmatic differentiation in

489 nature of course do not lend themselves to such a direct comparison (e.g. the Earth doesn't

490 produce rhyolites containing mostly MgO as the modifier oxide, instead of Na_2O) but

491 nonetheless such effects of composition should be inherent in any model of bulk

492 thermodynamics, phase equilibria, and magmatic properties. Models that treat all modifier oxide

493 components as equivalent must thus be only first approximations.

494

495 *Suppression of phase separation by alumina*

496 $\qquad$ When alumina is added to an alkali or alkaline earth binary silicate liquid, the negative

497 charges on NBO are spread out among multiple BO (Fig. 9, 10), resulting in less tendency for

498 clustering and ultimately less tendency for liquid-liquid phase separation. Two-liquid solvi are

499 greatly suppressed in all such ternary phase diagrams, and, instead of being nearly universal as in

500 binary silicate systems, often are reduced to no significance at all in the aluminosilicates that

501 comprise most magmas. Less clustering of modifier cations and NBO into "channels" is also a

22

502   consequence of alumina addition, expected to affect diffusivities significantly. In parallel, a great

503   deal of advanced technology also depends on this drastic effect of structure on phase diagrams,

504   for example the alkaline earth aluminoborosilicate glasses used in computer display screens.

505

506   *Potential for ordering among different modifier cations in aluminosilicate melts*

507   In compositions with total modifier oxide contents higher than alumina (e.g.

508   "peralkaline" compositions, and most "metaluminous" intermediate and mafic magmas), NBO

509   could be distributed over AlO_4 and/or SiO_4 groups. The latter generally "win", at least at the low

510   temperatures captured by glasses (Allwardt et al., 2003; Mysen, 1997). As discussed above for

511   simple Al-free melts, the non-network cations can be distributed in many different ways with

512   different combinations of NBO and BO neighbors, with the expectation that larger, lower

513   charged cations (e.g. alkalis) may be more likely to be coordinated by BO such as Si-O-Al and

514   smaller, higher charged cations (e.g. Mg^{2+}) may associate more with the NBO. This phenomenon

515   is clearly seen in some crystalline silicates. For example, in biotite, the higher field strength Mg^{2+}

516   and Fe^{2+} cations are coordinated only by NBO (and OH^-) in the octahedral sheets, while larger,

517   monovalent K^+ cations are surrounded by Si-O-Al BO in the interlayers. There is some evidence

518   for this kind of ordering in glasses (Allwardt and Stebbins, 2004; Kelsey et al., 2008; Mysen and

519   Richet, 2005); it provides another potential source of configurational entropy and heat capacity

520   on disordering above T_g. Furthermore, such energetic "preferences" of different cations in

521   different coordination environments must certainly matter in models of how they diffuse in

522   melts, of central importance to problems of crystal growth, melting, and mixing.

523

524   *Alumina content, viscosity, and variations from standard models of structure*

23

525   As more and more alumina is added to a simple binary silicate melt, the fraction of

526   oxygens that are NBO, and the NBO/T ratio, systematically decrease. The melt "fragility" and

527   configurational entropy decrease, and high temperature viscosity goes up. In the standard model

528   approximation, when the modifier oxide/alumina ratio is reduced to 1, all oxygens are bridging

529   and the composition of the melt will be along a "1:1" join such as SiO_2-$NaAlSiO_4$ or SiO_2-

530    $CaAl_2Si_2O_8$. As in the calculation of a CIPW norm, the local structure of such melts (e.g.

531   anhydrous high-silica rhyolites) can be approximated by locally feldspar- and silica-like

532   structures with some disorder in mixing of both charge compensating and network cations, bond

533   angles and ring sizes, etc. But how is it that such a "strong" liquid can flow at all? Both physical

534   property and structural data indicate that the dynamics of such BO-rich systems are particularly

535   sensitive to structural "imperfections", in particular the introduction of NBO and weakening of

536   BO links by fugitive and mobile components such as H_2O. Even anhydrous melts generate their

537   own "defects" that fall outside of standard structural models, however. For example, ^{17}O NMR

538   spectroscopy of glasses on 1:1 joins has shown that they *do* contain small amounts of NBO, and

539   these concentrations again are higher for higher charged modifiers (e.g. Ca^{2+} vs. K^+) (Thompson

540   and Stebbins, 2011). Such non-standard species may have important effects on transport

541   properties, and in fact were predicted from detailed studies of composition vs. viscosity in

542   ternary aluminosilicate melts (Mysen and Toplis, 2007; Toplis and Dingwell, 2004; Toplis et al.,

543   1997b).

544

545   **Al and Si coordination, network defects, and effects of pressure**

546   *The roles of non-tetrahedral Al and Si*

24

547   Another key approximation of standard models of glass and melt structure is that all Al^{3+}

548   cations have exactly four oxygen neighbors for compositions in which the modifier oxides

549   exceed or equal the alumina contents; formation of higher coordinated Al in peraluminous

550   composition has long been suggested to accommodate local charge balance, but such Al-rich

551   magmas are uncommon in nature. ^{27}Al NMR has now clearly shown that even in strongly

552   peralkaline (e.g. $Na_2O/Al_2O_3 \gg 1$) and "peralkaline earth" (e.g. $CaO/Al_2O_3 \gg 1$) ternary

553   aluminosilicate glasses, some five-coordinated Al (^{V}Al), and even some ^{VI}Al, are indeed present

554   (Kelsey et al., 2009a; McMillan and Kirkpatrick, 1992; Neuville et al., 2006; Neuville et al.,

555   2008b; Toplis et al., 2000). Once again, the field strength of the modifier cation has a big effect,

556   producing typically 5 to 8% ^{V}Al in the well-studied Ca aluminosilicates and even more in Mg

557   aluminosilicates. The formation of "non-standard" ^{V}Al may be related to that of "non-standard"

558   NBO, but there is not a simple 1 to 1 relationship (Thompson and Stebbins, 2011). Both

559   probably increase with increasing T above T_g, contributing further to the configurational entropy

560   and to reducing the "strength" of the liquid (Stebbins et al., 2008). X-ray and neutron scattering

561   methods, applied to aluminosilicate glasses and even in-situ to high temperature melts, are also

562   important in observing and modeling deviations from the conventional structural picture

563   (Guignard and Cormier, 2008; Jakse et al., 2012; Neuville et al., 2008a).

564   Five-coordinated network cations (^{V}Al and ^{V}Si), and the longer, weaker bonds that go

565   with them, have long been suggested as "transition states" or "reaction pathways" in the local

566   bond-breaking and rearrangement that must occur for viscous flow, and diffusion of Si, Al, and

567   O, to happen in such highly connected structures (Fig. 11). This was suggested by early

568   computer simulations of melts (Angell et al., 1982; Brawer, 1985). The discovery of small

569   concentrations of ^{V}Si even in low-pressure alkali silicate glasses (Stebbins and McMillan, 1993),

25

570 and now of much more abundant ^{V}Al, has been particularly interesting for this reason. As Earth

571 scientists know so well, both Si and Al coordination increases in *crystalline* silicates (most

572 commonly to the six-coordinated structures, of course) are fundamental in high pressure

573 transformations in the deep crust and mantle. Intriguingly, some of the first indirect evidence for

574 such coordination shifts in silicate *melts* came from anomalous viscosity *decreases* with

575 increasing pressure of relatively "strong" compositions such as $K_2Si_4O_9$ and $NaAlSi_2O_6$ (Angell

576 et al., 1982; Wolf and McMillan, 1995). These contrast with the *increases* in viscosity with

577 pressure expected for "normal" liquids simply because of density increase and tighter ionic

578 packing. The latter behavior is indeed seen for "weaker" silicate melts such as $CaMgSi_2O_6$ and

579 mafic basalts (Liebske et al., 2005). Although quantifying the interplay of network cation

580 coordination and melt viscosity remains elusive, it is an intriguing issue for rationalizing both

581 compositional and pressure effects on this petrologically critical property, which can vary over at

582 least 12 orders of magnitude in natural silicate liquids.

583   As in minerals, the most obvious connection between pressure-induced increases in Al

584 and/or Si coordination in silicate melts and their properties is through density or molar volume.

585 Radical changes in structure of simple oxide and silicate glasses at lower mantle pressures have

586 been reported from in-situ diffraction and spectroscopic studies (Farber and Williams, 1996;

587 Majérus et al., 2004; Wolf and McMillan, 1995), but glasses compressed under such conditions

588 may revert at least partially on decompression to lower-pressure structures, making more

589 detailed structural studies difficult. Nonetheless, it is likely that at very high pressures (>30

590 GPa?), Si and Al cations in melts all have six oxygen neighbors, and behave more like dense

591 ionic liquids than the strongly connected network liquids that are familiar to us at near-surface

592 pressures.

26

593   At more modest pressures (to at least 10-12 GPa, representing deeper regions of the

594   Earth's upper mantle), many silicate and aluminosilicate melts can be quenched to glasses, which

595   can then be decompressed for detailed structural studies at room temperature and pressure. These

596   densified glasses may be up to 15 to 20% denser than the same glass initially melted at 1 bar. In

597   one recent study of aluminosilicates similar in composition to rhyolitic to intermediate magmas

598   (Malfait et al., 2014), melt densities measured by in-situ X-ray methods to 3.5 GPa were

599   compared to those calculated from recovered glass density and its measured elastic constants.

600   Agreement within uncertainties in the experimental measurements involved suggested that

601   inelastic volume relaxation during decompression of the glass at room temperature was not

602   important, and thus that the recovered glass structure was a good representation of the melt

603   structure at high pressure and T_g. Other very recent studies (Bista et al., 2015; Gaudio et al.,

604   2015) have also shown, however, that significant, transient pressure drops can take place on

605   quenching of a high temperature melt in a solid medium high pressure apparatus, and that

606   experiments with initial temperatures near to T_g will retain greater structural and density

607   changes, if crystallization can be avoided. Many published estimates of structural changes in

608   glasses quenched from high pressure may thus be minimum values. In any case, Al-free alkali

609   silicate glasses quenched from melts initially at 10 to 12 GPa contain up to at least 15% of ^{V}Si

610   and ^{VI}Si (Allwardt et al., 2004; Gaudio et al., 2008; Xue et al., 1991). NBO-rich aluminosilicate

611   compositions, which are about 95% ^{IV}Al when melted at 1 bar, can be recovered from 6 to 10

612   GPa with the *majority* of Al converted to ^{V}Al and ^{VI}Al (Kelsey et al., 2009a). As noted above for

613   1 bar glasses, higher field strength modifier cations ($Mg^{2+} > Ca^{2+} > Na^+ > K^+$) greatly promote

614   the formation of higher coordinated Al at high pressure, but such effects on Si coordination are

615   much less well known (Allwardt et al., 2005; Kelsey et al., 2009b). There is good evidence that

27

616 a relatively easy pathway for conversion of both ^{IV}Si and ^{IV}Al to higher coordination involves

617 conversion of NBO to "bridging" or "intermediate" oxygen links involving the higher

618 coordinated cations (Allwardt et al., 2004; Lee et al., 2004; Yarger et al., 1995). Thus, such

619 changes in NBO-poor liquids (e.g. rhyolites in contrast to basalts) probably happen more

620 gradually, by different mechanisms, and at higher pressures. The most common magmas formed

621 in the mantle of the modern Earth are mafic basalts, which not only have high proportions of

622 NBO but high concentrations of high field strength cations (notably Mg^{2+} and Fe^{2+}), which will

623 both promote coordination increase of at least Al. Recent studies indicate that even at the

624 "modest" upper mantle pressures where most basaltic magmas commonly arise (say, 2-3 GPa),

625 high concentrations of ^{V}Al and even ^{VI}Al are present, which may have to be considered in

626 refinements of models of melt properties (Bista et al., 2015).

627   As mentioned above, species such as ^{V}Al and ^{V}Si have been implicated in mechanisms of

628 viscous flow and the diffusion of network components in melts, and this role may be accentuated

629 at higher pressures. In fact, ^{V}Si or ^{VI}Si-rich melts may become so "fragile" that they can't be

630 readily quenched to glasses, placing limits on what can be recovered for ex-situ spectroscopy.

631 What about the most obviously expected high pressure property change, namely density? In

632 recovered glasses that do contain measurable amounts of high-coordinated Al and/or Si, the

633 effects of this structural change can be compared with measured density increases in the glasses,

634 by using models of partial molar volumes of oxide components and substituting, for example, a

635 "corundum-like" volume for alumina. It has been found that even in the most densified, ^{V}Al- and

636 ^{VI}Al-rich glasses, this observed structural change can account for only a relatively minor part of

637 the density increase (Allwardt et al., 2005). Most of the densification in this pressure range is

638 probably thus accommodated by compression of "softer" cation sites, i.e. those of the modifier

28

639   cations, and some accompanying topological reconfiguration of the network. We have hints

640   about these kinds of changes from apparent reductions in network bond angles (Mysen and

641   Richet, 2005) and in ^{23}Na NMR spectra suggesting smaller Na sites (Kelsey et al., 2009a), but a

642   detailed picture of this process remains to be determined. The development of abundant high-

643   coordinated Al and Si at high pressure also will greatly alter the oxygen speciation in the

644   network, will contribute to increased configurational complexity, and is expected to have major

645   effects on thermodynamic and transport properties (Lee, 2004; Lee et al., 2004).

646

647   *Alumina activity and Al coordination?*

648   As discussed above for silica activity, compositional effects on the local structural

649   environments of Al^{3+} cations should have effects on component activities. It might be expected,

650   for example, that the formation of more highly coordinated Al would increase the activity of melt

651   components related to the formation of minerals containing ^{VI}Al. Accurate data on the 1-bar

652   liquidus surfaces for such phases, such as corundum and mullite, are limited, so that it is difficult

653   to make the sort of direct comparison of the effects of, say, modifier cation field strength, as

654   were described above for a_{SiO2}. Such equilibria are even more poorly constrained at high

655   pressures where high coordinated Al becomes abundant. However, the Al_2O_3 component in a

656   model such as pMELTS (Ghiorso et al., 2002) may represent the activity of non-tetrahedral Al,

657   as tetrahedral Al can be accounted for by feldspar or feldspathoid-like components. Alumina

658   activity is constrained at least in part by high pressure liquid-crystal equilibria with ^{VI}Al-

659   containing phases such as spinels and Al-rich pyroxenes, even in the metaluminous compositions

660   that comprise most of the model data base. If this is the case, then known systematic effects of

661   modifier cation field strength on Al coordination might be expected to systematically change

29

662   a_{Al2O3}. Using the same "isochemical" substitutions of MgO vs. FeO vs. CaO vs. Na_2O vs. K_2O as

663   described above for silica, this correlation is indeed found (Fig. 8). This structure-activity

664   correlation is admittedly speculative, but suggests that direct experiments with well-constrained

665   phase equilibria in simple peraluminous systems could be worth attempting.

666   Models of melt properties based on "non-structural" oxide components, or on simple low

667   pressure mineral components, will become more and more difficult to accurately constrain at

668   higher and higher pressures. The need for multicomponent models that explicitly account for

669   major structural changes (notably in Si coordination) has been recognized and important steps

670   made in their formulation (Ghiorso, 2004). At this time the structural "data" for these models has

671   come largely (and necessarily) from computer simulations; we might hope that in the future more

672   data from both ex-situ and in-situ structural measurements will become available to constrain

673   such petrologically important computational tools.

674

675   **Pressure effects on melt structure and properties: insights from non-silicate analog systems**

676   Two other well-studied families of glass-forming oxide melts may provide some

677   qualitative insights into some of the composition/structure/property effects to be expected in high

678   pressure aluminosilicates (Stebbins et al., 2013). In contrast to silicon in simple silicates at 1 bar

679   pressure, boron in binary borate crystals and melts has two coordination states with oxygen, ^{III}B

680   and ^{IV}B, that are energetically close enough so that both can readily form. In germanate melts

681   and crystals, structures with ^{IV}Ge, ^{V}Ge, and ^{VI}Ge are all readily accessible at 1 bar. In both

682   systems, the binaries with alkali oxides have the widest glass-forming ranges and are most fully

683   studied. In both cases, the pure network forming glass (B_2O_3, GeO_2) is known to contain only the

684   low coordination state (^{III}B, ^{IV}Ge). As alkali oxide is added, the initial structural change is *not* to

30

685   primarily form NBO as in silicates, but to accommodate the added oxide ion by increasing the

686   coordination of the network cation (^{IV}B and ^{V,VI}Ge), illustrated by Figure 4b. This is found in

687   liquids, glasses, and crystals out to roughly 20 mol% added modifier oxide. To this point, the

688   modifier cations are coordinated primarily by bridging oxygens, some of which will have partial

689   negative charges, e.g. $[^{III}B–O–^{IV}B]^{-1/4}$ or $[^{IV}Ge–O–^{V}Ge]^{-1/5}$. At alkali oxide higher contents,

690   NBO *do* begin to form and the network cation coordination goes back down, eventually to again

691   being dominated by the low coordination numbers. The variation with composition in melt and

692   glass properties, such as viscosity, T_g, and most obviously molar volume, is highly non-linear

693   because of these complex structural changes (Stebbins et al., 2013), and are often analyzed with

694   models containing multiple components representing different local structures. These kinds of

695   systems may represent some of the complex effects of changing composition in aluminosilicate

696   melts at intermediate pressures where more than one coordination of Si or Al can readily form,

697   and again, point out the possible complexity of models needed to accurately capture non-linear

698   property variation. To date however, the experimental data sets for neither high pressure melt

699   properties nor structure are wide enough in scope to begin to define such transitions. As

700   suggested by the 2-D analog portrayed in Figure 6, a shift with pressure from primarily ^{IV}Al and

701   ^{IV}Si to a mix with ^{V,VI}Al and ^{V,VI}Si is also expected to have large effects on the configurational

702   entropy, the dispersion vs. concentration of charges on oxygen species, liquid immiscibility, and

703   heterogeneity/homogeneity of modifier cation distribution.

704

705   **Melt disorder and the roots of magmatic phase equilibria**

706   As mentioned above, we now have qualitative, and in many cases quantitative insights

707   into many different, if inter-related, aspects of structural disorder in silicate glasses and melts,

31

708   and, in some cases, to how this increases with temperature. These include ordering/disordering of

709   different network modifying/charge compensating cations (e.g. Na^+, Ca^{2+}, Mg^{2+}, Fe^{2+}) in sites

710   with varying oxygen coordination, of different types of network forming cations (e.g. Si^{4+}, Al^{3+})

711   and of the consequent different types of bridging oxygens, of NBO and BO, and even of varying

712   coordination states of Si and Al. It is likely that other less readily measurable contributions to

713   disorder, for example the high energy defects that must be formed in higher and higher

714   concentrations as cations diffuse more and more rapidly, make important contributions to

715   configurational properties in melts, but as yet are poorly characterized (Stebbins, 2008).

716   Nonetheless, it is clear that many potential sources of structural disorder in melts, and for

717   increases in disorder with temperature, increase as the "simple" network of pure silica is broken

718   apart by modifier oxides. Apart from obvious effects on melt fragility and hence on diffusivity

719   and viscosity, one outcome is a systematic increase in enthalpies and entropies of fusion of

720   silicate minerals as the fraction of non-bridging oxygens increases (Richet and Bottinga, 1986;

721   Stebbins et al., 1984). Large differences can also be seen among ΔS_m even for oxides of simple

722   compositions, which are also obviously related to their network-forming ability. For partially

723   covalent, network-forming SiO_2, ΔS_m is the lowest known (1.5 J/K/mole of atoms), contrasting

724   with estimated values for oxides of larger tetravalent cations such as TiO_2 (9.9 J/K/mole of atoms

725   (Chase et al., 1985)) and ZrO_2 (9.8 J/K/mole of atoms) which form liquids with higher cation and

726   anion coordination, longer bonds, and more ionic interactions.

727   As pointed out in the ground-breaking igneous petrology textbook of Carmichael, Turner

728   and Verhoogen (Carmichael et al., 1974), a simple calculation of binary phase diagrams suggests

729   that this relationship between what are now known as structural differences, and the silica

730   content of the crystal and melt, has fundamental consequences for magmatic phase equilibria. If

32

731   we assume no solid solution, and ideal solution in the liquid (often very rough assumptions, but

732   useful in this context), the equilibrium constant for melting of a single mineral component i

733   simply becomes the mole fraction of i in the liquid, $X_{i,Liq}$. With the further approximations of

734   constant ΔH_m (and thus ΔS_m) of melting, the Van't Hoff equation gives:

735             $$d (\ln X_{i,Liq})/dT \ = \ \Delta H_m/(RT^2) \qquad\qquad\qquad (7)$$

736   Simply inverting to examine the effects of dilution of component i in the liquid (i.e. how much

737   does the liquidus temperature drop as other components are added to the melt), it is easy to see

738   that, with all else equal, a mineral with a small enthalpy and entropy of fusion, and thus greatest

739   mineral-melt structural similarity, will have a liquidus curve that drops more steeply with

740   decreasing X_i than that of a mineral with a high enthalpy and entropy of fusion, and thus greatest

741   melt disorder relative to crystal. Eutectic temperatures are thus lowered and eutectic

742   compositions (the last liquid to crystallize or the first liquid produced on melting) are enriched in

743   the components with smaller ΔH_m and ΔS_m (Fig. 12). Given that the silica polymorphs, and

744   alkali feldspars as well, have much lower ΔH_m and ΔS_m values than mafic silicates such as Mg-

745   rich olivines and pyroxenes, it is thus not surprising that most natural magmas become enriched

746   with silica and alkali feldspar components as they differentiate, as these minerals generally come

747   into equilibrium only at low temperatures at high concentrations of these components. Of course

748   real magmatic phase equilibria are highly complex and often involve highly non-ideal solutions

749   in both liquids and solids, but the steep liquidus curve for silica, required by its low ΔH_m and

750   ΔS_m, must be a key part of the eventual enrichment of magmas in silica and the low temperature

751   of appearance of silica phases in magmas, in spite of the relatively high pure-phase melting point

752   of silica. In fact, the overall progressions in the succession of minerals to form during

753   differentiation, as summarized by Bowen's reaction series, from olivines to pyroxenes to sheet

33

754 silicates and from Ca rich to Na, K rich feldspars and eventually quartz, can in some sense be

755 viewed as a progression from the crystallization of highly disordered melt components to highly

756 ordered components. There are thus deep melt structural roots to the most basic of natural

757 magmatic processes.

758

759 **Structure and dynamic processes in melts**

760 Fundamental connections between melt structure and viscosity, as illustrated by the

761 Adam-Gibbs relationship between the shape of the viscosity curve and configurational entropy,

762 (eq. 1) have already been made above. In silicate melts, knowledge is still very limited on the

763 mechanistic details of links between non-vibrational atomic motions, such as cation site hopping,

764 bond breaking and re-arrangement, and petrologically crucial processes of viscous flow and

765 diffusion. Many ideas about these links have come, and will continue to come, from atomistic

766 computer simulations, often termed "molecular dynamics" (MD, although this label is not so

767 appropriate for mostly non-molecular silicate liquids) but space does not allow detailed

768 discussion of this important field (Ghosh et al., 2014; Guillot and Sator, 2007; Martin et al.,

769 2009; Stixrude et al., 2009). A few examples of experimental insights will be given here, along

770 with some basic theoretical concepts.

771 One key concept is the "shear relaxation time" (τ_s) for a liquid, for which an average

772 value can be estimated from the "Maxwell" equation (Dingwell, 2006; Dingwell and Webb,

773 1990; Mysen and Richet, 2005), the viscosity, and the infinite frequency shear modulus G_∞. The

774 latter represents deformation going on at very short length scales in the melt, and is typically

775 about 1 to 3×10^{10} Pa in molten silicates:

776 $\qquad \tau_s = \eta / G_\infty$ $\hspace{8cm}$ (8)

34

777   τ_s, although based on macroscopic measurements, is often presumed to be some measure the

778   inverse of the rate of some small-scale dynamic process (or processes) that controls viscous flow.

779   Estimated values of τ_s vary just as widely as do those for viscosity in magmas, for example a few

780   nanoseconds in an alkali basalt near its liquidus ($\eta = 10^1$ Pa$^.$s) to a few seconds in a rhyolite

781   dome ($\eta = 10^{11}$ Pa$^.$s). In a few cases, we actually have quantitative data on the average lifetimes

782   of small-scale structural units in simple molten silicates, such as Q^n species and BO vs. NBO. As

783   Si-O bonds break and rearrange during flow (and the closely related process of diffusion of these

784   network ions), these local species exchange back and forth, as illustrated in an MD-inspired

785   cartoon view in Figure 11. In situ, high temperature NMR data has measured these rates in a few

786   alkali silicate liquids with relatively high silica contents, and they can be close to the inverse of

787   τ_s estimated from the Maxwell equation (Farnan and Stebbins, 1990; Farnan and Stebbins, 1994;

788   Sen, 2008; Stebbins et al., 1995b). The fundamental conclusion here is that although the concept

789   of "polymerization" is deeply embedded in the glass structure literature as a description of the

790   extent of network connectivity, the silicate melts for which we have data do not dynamically

791   behave anything like organic polymers, whose viscosities are primarily controlled by the

792   coordinated motions of large, weakly interacting molecules. These are built with strong carbon-

793   carbon bonds whose lifetimes are vastly longer than the time scale set by τ_s. This view is

794   supported by a few measurements of silicates and borates that show no retention of local

795   structural alignment of structural groups when rapidly deformed during cooling to glass

796   (Stebbins et al., 1989; Wu et al., 2009), again in stark contrast to organic polymers. It is possible

797   that in much lower silica liquids, viscous flow may be dominated by breaking and re-forming of

798   weaker bonds among NBO and modifier cations, with longer-lasting Si-O bonds in small

799   "molecule-like" fragments, but as yet we have almost no experimental data in such systems.

35

800   If viscous flow is closely linked to the rate of network bond breaking, then it should also

801   be closely related to tracer diffusion of *network* cations and anions. In fact, such relationships are

802   often at least approximately seen in silicate melts (within better than a $\log_{10}$ unit), through

803   analysis of data using the Eyring equation, that links the diffusion constant D to atomic site

804   hopping at a mean timescale of τ_E and a jump distance of d. For network species τ_E is expected

805   to be closely related to τ_s and d to a typical Si-Si or O-O distance:

806          $D = d^2/6\tau_E$ (9)

807   The "Einstein –Smoluchowski" relationship connects viscosity to network ion diffusivity directly

808   (Stebbins, 1995), given k_B as the Boltzmann constant:

809          $\eta = k_B T/dD$ (10)

810   In fact, measurements of diffusivities of Si and/or of O can be used as at least rough proxies of

811   melt viscosity, when the latter can be very challenging to measure, for example at high pressure

812   (Poe et al., 1997; Reid et al., 2003; Tinker et al., 2004). Si and O atomic motions can thus be

813   described as highly "coupled" to network structural dynamics.

814   In contrast, weakly bonded network modifier cations, most notably the alkalis, can move

815   about in the melt much more rapidly, and can be considered to be "decoupled" from the network.

816   Long-range diffusion of weakly bonded ions may be facilitated if NBO are concentrated in

817   domains or channels that allow "percolation" through the network, rather than being dispersed

818   evenly with BO (Greaves and Sen, 2007) (Fig. 6 vs. Fig. 10). The formation of this kind of

819   "intermediate-range" structure is related to the same interactions that can give rise to liquid-

820   liquid phase separation, as discussed above. Network bond breaking "freezes out" at the glass

821   transition. However, rapid diffusion of alkalis at temperatures well below T_g may be important

822   not only in geochemical processes, but is at the heart of technologies involving Li-ion

36

823   conducting glasses and the alkali exchange employed in the chemical tempering of glass sheets

824   made to protect mobile phone displays. Network modifier cations with higher charge, notably

825   Mg^{2+}, Ca^{2+}, and Fe^{2+} in magmas, may have intermediate dynamical behavior, with diffusive time

826   scales coupled to those of the network at higher temperature, but "decoupling" at lower

827   temperature (George and Stebbins, 1998).

828   In multicomponent, "chemical" diffusion that is so important in transporting the building

829   blocks of crystals and in homogenizing liquids after melting and mixing, complex interactions

830   among components are expected through mutual effects on chemical potentials, the need for

831   local as well as overall charge balance. These may appear as correlations among diffusivities that

832   can seem to suggest the diffusion of larger structural units, e.g. "molecules" of feldspar. Given

833   the close relationship of network bond breaking, viscous flow, and network tracer diffusivities

834   noted above, it seems unlikely that the lifetime of such multi-cation structural units is long

835   enough for them to move, intact, for significant distances. However, just as mineral-like

836   components have long been useful in models of free energies and phase equilibria in melts,

837   correlated grouping of atoms may be useful in models of diffusion to capture some of the

838   dynamical consequences of short-range structural interactions.

839

840   **Implications and prognosis**

841   Most silicate melts in nature have large "configurational" components to their

842   thermodynamic properties, meaning that structural changes with pressure, composition and

843   temperature have direct relationships to petrological processes from melting and crystallization

844   to temperature and pressure-caused density changes. The differences in entropies and enthalpies

845   of fusion among various silicate minerals, which exert a first-order control on magmatic phase

37

846   equilibria, have obvious relationships to differences in melt structure. Links between melt

847   structure and magmatic transport properties, including diffusion and viscous flow, are also

848   fundamental. Many of these connections are now beginning to be understood at a qualitative and

849   sometimes quantitative level, and should be useful concepts to those working on the complex

850   realities of magmatic systems in both nature and the laboratory, to guide interpretations of data

851   and help to formulate more physically-based models. In turn, the questions and phenomena of

852   petrology should inform ongoing directions of structural studies. There is a bright future for

853   experimental and theoretical work on melt structure and processes, both through the relatively

854   accessible "window" provided by quenched, glassy samples, and in the challenging world of in-

855   situ, high temperature and high pressure measurements.

856

862

863

References

864

865 Allwardt, J.R., Lee, S.K., and Stebbins, J.F. (2003) Bonding preferences of non-bridging

866 oxygens in calcium aluminosilicate glass: evidence from ^{17}O MAS and 3QMAS NMR on

867 calcium aluminate and low-silica Ca-aluminosilicate glasses. American Mineralogist, 88, 949-

868 954.

869 Allwardt, J.R., Schmidt, B.C., and Stebbins, J.F. (2004) Structural mechanisms of compression

870 and decompression in high pressure $K_2Si_4O_9$ glasses: An investigation utilizing Raman and

871 NMR spectroscopy of high-pressure glasses and crystals. Chemical Geology, 213, 137-151.

872 Allwardt, J.R., and Stebbins, J.F. (2004) Ca-Mg and K-Mg mixing around non-bridging oxygens

873 in silicate glasses: An investigation using oxygen-17 MAS and 3QMAS NMR. American

874 Mineralogist, 89, 777-784.

875 Allwardt, J.R., Stebbins, J.F., Schmidt, B.C., Frost, D.J., Withers, A.C., and Hirschmann, M.M.

876 (2005) Aluminum coordination and the densification of high-pressure aluminosilicate glasses.

877 American Mineralogist, 90, 1218-1222.

878 Angell, C.A. (1985) Strong and fragile liquids. In K.L. Ngai, and G.B. Wright, Eds. Relaxation

879 in Complex Systems, p. 3-11. Office of Naval Research, Washington.

880 Angell, C.A., Cheeseman, P.A., and Tamaddon, S. (1982) Pressure enhancement of ion

881 mobilities in liquid silicates from computer simulation studies to 800 kilobars. Science, 218,

882 885-887.

883 Bista, S., Stebbins, J.F., Hankins, B., and Sisson, T.W. (2015) Aluminosilicate melts and glasses

884 at 1 to 3 GPa: Temperature and pressure effects on recovered structural and density changes.

885 American Mineralogist, in press.

39

886   Brawer, S. (1985) Relaxation in Viscous Liquids and Glasses. American Ceramic Society, Inc.,

887   Columbus.

888   Brown, G.E., Jr., Farges, F., and Calas, G. (1995) X-ray scattering and x-ray spectroscopy

889   studies of silicate melts. In J.F. Stebbins, P.F. McMillan, and D.B. Dingwell, Eds. Structure,

890   Dynamics, and Properties of Silicate Melts, 32, p. 317-410. Mineralogical Society of

891   America, Washington, D.C.

892   Brown, I.D., and Shannon, R.D. (1973) Empirical bond-strength - bond-length curves for oxides.

893   Acta Crystallographica, A29, 266-282.

894   Calas, G., Henderson, G.S., and Stebbins, J.F. (2006) Glasses and melts: linking geochemistry

895   and materials science. Elements, 2, 265-268.

896   Carmichael, I.S.E., Turner, F.J., and Verhoogen, J. (1974) Igneous petrology. 739 p. McGraw-

897   Hill, New York.

898   Chase, M.W., Davies, C.A., Downey, J.R., Jr., Frurip, D.J., McDonald, R.A., and Syverud, A.N.

899   (1985) JANAF Theromochemical Tables, Third Edition. American Institute of Physics, New

900   York, NY.

901   Cormier, L., and Cuello, G.J. (2013) Structural investigation of glasses along the $MgSiO_3$-

902        $CaSiO_3$ join: diffraction studies. Geochimica et Cosmochimica Acta, 122, 498-510.

903   Davis, M.C., Sanders, K.J., Grandinetti, P.J., Gaudio, S.J., and Sen, S. (2011) Structural

904   investigations of magnesium silicate glasses by ^{29}Si 2D magic-angle flipping NMR. Journal of

905   Non-Crystalline Solids, 357, 2787-2795.

906   deJong, B.H.W.S., and Brown, G.E., Jr. (1980) Polymerization of silicate and aluminate

907   tetrahedra in glasses, melts and aqueous solutions-II. The network modifying effects of Mg^{2+},

40

908   K^+, Na^+, Li^+, OH^-, F^-, Cl^-, H_2O, CO_2 and H_3O^+ on silicate polymers. Geochimica et

909   Cosmochimica Acta, 44, 1627-1642.

910   Dingwell, D.B. (2006) Transport properties of magmas: diffusion and rheology. Elements, 2,

911   281-286.

912   Dingwell, D.B., and Webb, S.L. (1990) Relaxation in silicate melts. European Journal of

913   Mineralogy, 2, 427-449.

914   Dirken, P.J., Kohn, S.C., Smith, M.E., and van Eck, E.R.H. (1997) Complete resolution of Si-O-

915   Si and Si-O-Al fragments in an aluminosilicate glass by ^{17}O multiple quantum magic angle

916   spinning NMR spectroscopy. Chemical Physics Letters, 266, 568-574.

917   Dubinsky, E.V., and Stebbins, J.F. (2006) Quench rate and temperature effects on framework

918   ordering in aluminosilicate melts. American Mineralogist, 91, 753-761.

919   Farber, D.L., and Williams, Q. (1996) An in-situ Raman spectroscopic study of $Na_2Si_2O_5$ at high

920   pressures and temperatures: Structures of compressed liquids and glasses. American

921   Mineralogist, 81, 273-283.

922   Farges, F., Brown, G.E., Jr., Calas, G., Galoisy, L., and Waychunas, G.A. (1994) Temperature-

923   induced structural transformations in Ni-bearing silicate glass and melt. Geophysical Research

924   Letters, 21, 1931-1934.

925   Farges, F., Brown, G.E., Navrotsky, A., Gan, H., and Rehr, J.R. (1996) Coordination chemistry

926   of Ti(IV) in silicate glasses and melts. 3. Glasses and melts from ambient to high

927   temperatures. Geochimica et Cosmochimica Acta, 60, 3055-3065.

928   Farnan, I., and Stebbins, J.F. (1990) A high temperature ^{29}Si NMR investigation of solid and

929   molten silicates. Journal of the American Chemical Society, 112, 32-39.

930   -. (1994) The nature of the glass transition in a silica-rich oxide melt. Science, 265, 1206-1209.

41

931   Galoisy, L. (2006) Structure-property relationships in industrial and natural glasses. Elements, 2,

932   293-297.

933   Gatti, C., Ottonello, G., and Richet, P. (2012) Energetics and bonding in aluminosilicate rings

934   with alkali metal and alkaline-earth metal charge-compensating cations. Journal of Physical

935   Chemistry A, 116, 8584-8598.

936   Gaudio, S.J., Lesher, C.E., Maekawa, H., and Sen, S. (2015) Linking high-pressure structure and

937   density of albite liquid near the glass transition. Geochimica et Cosmochimica Acta, in press.

938   Gaudio, S.J., Sen, S., and Lesher, C.E. (2008) Pressure-induced structural changes and

939   densification of vitreous $MgSiO_3$. Geochimica et Cosmochimica Acta(72), 1222-1230.

940   George, A.M., and Stebbins, J.F. (1998) Structure and dynamics of magnesium in silicate melts:

941   a high temperature [25]Mg NMR study. American Mineralogist, 83, 1022-1029.

942   Ghiorso, M.S. (2004) An EOS for silicate melts. III. Analysis of stoichiometric liquids at

943   elevated pressure: shock compression data, molecular dynamics simulations and mineral

944   fusion curves. American Journal of Science, 304, 752-810.

945   Ghiorso, M.S., Hischmann, M.M., Reiners, P.W., and Kress, V.C. (2002) The pMelts: A revision

946   of MELTS for improved calculation of phase relations and major element partitioning related

947   to partial melting of the mantle to 3 GPa. Geochemistry Geophysics Geosystems, 3, 1030.

948   Ghosh, D.B., Karki, B.B., and Stixrude, L. (2014) First-principles molecular dynamics

949   simulations of $MgSiO_3$ glass: structure, density and elasticity at high pressure. American

950   Mineralogist, 99, 1304-1314.

951   Giordano, D., Mangiacapra, A., Potuzak, M., Russell, J.K., Romano, C., Dingwell, D.B., and Di

952   Muro, A. (2006) An expanded non-Arrhenian model for silicate melt viscosity: A treatment

953   for mataluminous, peralumuninous, and peralkaline liquids. Chemical Geology, 229, 42-56.

42

954 Greaves, G.N., and Sen, S. (2007) Inorganic glasses, glass-forming liquids and amorphizing

955   solids. Advances in Physics, 56, 1-166.

956 Guignard, M., and Cormier, L. (2008) Environments of Mg and Al in MgO-Al_2O_3-SiO_2 glasses:

957   A study coupling neutron and X-ray diffraction and Reverse Monte Carlo modeling. Chemical

958   Geology, 256, 111-118.

959 Guillot, B., and Sator, N. (2007) A computer simulation study of natural silicate melts. Part II:

960   high pressure properties. Geochimica et Cosmochimica Acta, 71, 4538-4556.

961 Gurman, S.J. (1990) Bond ordering in silicate glasses: a critique and re-solution. Journal of Non-

962   Crystalline Solids , 125, 151-160.

963 Henderson, G.S., Calas, G., and Stebbins, J.F. (2006) The structure of glasses and melts.

964   Elements, 2, 269-274.

965 Hess, K.U., Dingwell, D.B., and Rössler, E. (1996) Parameterization of viscosity-temperature

966   relations of aluminosilicate melts. Chemical Geology, 128, 155-163.

967 Hess, P.C. (1995) Thermodynamic mixing properties and structure of silicate melts. In J.F.

968   Stebbins, P.F. McMillan, and D.B. Dingwell, Eds. Structure, Dynamics, and Properties of

969   Silicate Melts, p. 145-189. Mineralogical Society of America, Washington, D.C.

970 Jakse, N., Bouhadja, M., Kozaily, J., Drewitt, J.W.E., Hennet, L., Neuville, D.R., Fischer, H.E.,

971   Cristiglio, V., and Pasturel, A. (2012) Interplay between non-bridging oxygen, triclusters, and

972   fivefold Al coordination in low silica content calcium aluminosilicate melts. Applied Physics

973   Letters, 101, 201903-1-5.

974 Kelsey, K.E., Allwardt, J.R., and Stebbins, J.F. (2008) Ca-Mg mixing in aluminosilicate glasses:

975   An investigation using [17]O MAS and 3QMAS and ^{27}Al MAS NMR. American Mineralogist,

976   93, 134-143.

977   Kelsey, K.E., Stebbins, J.F., Mosenfelder, J.L., and Asimow, P.D. (2009a) Simultaneous

978   aluminum, silicon, and sodium coordination changes in 6 GPa sodium aluminosilicate glasses.

979   American Mineralogist, 94, 1205-1215.

980   Kelsey, K.E., Stebbins, J.F., Singer, D.M., Brown, G.E., Jr., Mosenfelder, J.L., and Asimow,

981   P.D. (2009b) Cation field strength effect on high pressure aluminosilicate glass structure:

982   Multinuclear NMR and La XAFS results. Geochimica et Cosmochimica Acta, 73, 3914-3933.

983   Koroleva, O.N., Anfilogov, V.N., Shatskiy, A., and Litasov, K.D. (2013) Structure of Na2O-

984   SiO2 melt as a function of composition: In situ Raman spectroscopic study. Journal of Non-

985   Crystalline Solids, 375, 62-68.

986   Lee, S.K. (2004) Structure of silicate glasses and melts at high pressure: quantum chemical

987   calculations and solid-state NMR. Journal of Physical Chemistry B, 108, 5889-5900.

988   Lee, S.K., Cody, G.D., Fei, Y., and Mysen, B.O. (2004) Nature of polymerization and properties

989   of silicate melts and glasses at high pressure. Geochimica et Cosmochimica Acta, 68, 4189-

990   4200.

991   Lee, S.K., and Kim, E.J. (2014) Probing metal-bridging oxygen and configurational disorder in

992   amorphous lead silicates: In sights from ^{17}O solid-state nuclear magnetic resonance. Journal of

993   Physical Chemistry C, 119, 748-756.

994   Lee, S.K., and Stebbins, J.F. (2000) The structure of aluminosilicate glasses: high-resolution 17O

995   and 27Al MAS and 3QMAS NMR study. Journal of Physical Chemistry B, 104, 4091-4100.

996   Liebske, C., Schmickler, B., Terasaki, H., Poe, B.T., Suzuki, A., Funakoshi, K., Ando, R., and

997   Rubie, D.C. (2005) Viscosity of peridotite liquid up to 13 GPa: Implications for magma ocean

998   viscosities. Earth and Planetary Science Letters, 240, 589-604.

44

999   Maekawa, H., Maekawa, T., Kawamura, K., and Yokokawa, T. (1991) The structural groups of

1000   alkali silicate glasses determined from ^{29}Si MAS-NMR. Journal of Non-Crystalline Solids ,

1001   127, 53-64.

1002   Majérus, O., Cormier, L., Itié, J.-P., Galoisy, L., Neuville, D.R., and Calas, G. (2004) Pressure-

1003   induced Ge coordination change and polyamorphism in SiO_2-GeO_2 glasses. Journal of Non-

1004   Crystalline Solids, 345&346, 34-38.

1005   Malfait, W.J., Halter, W.E., Morizet, Y., Meier, B.H., and Verel, R. (2007a) Structural control on

1006   bulk melt properties: Single and double quantum ^{29}Si NMR spectroscopy on alkali-silicate

1007   glasses. Geochimica et Cosmochimica Acta, 71, 6002-6018.

1008   Malfait, W.J., Seifert, R., and Sanchez-Valle, C. (2014) Densified glasses as structural probes for

1009   high-pressure melts: configurational compressibility of silicate melts retained in quenched and

1010   decompressed glasses. American Mineralogist, 99, 2142-2145.

1011   Malfait, W.J., Zakaznova-Herzog, V.P., and Halter, W.E. (2007b) Quantitative Raman

1012   spectroscopy: High-temperature speciation of potassium silicate melts. Journal of Non-

1013   Crystalline Solids, 353, 4029-4042.

1014   Martin, G.B., Spera, F.J., Ghiorso, M.S., and Nevins, D. (2009) Structure, thermodynamic, and

1015   transport properties of molten Mg_2SiO_4: dynamics simulations and model EOS. American

1016   Mineralogist, 94, 693-703.

1017   Mauro, J.C., Yue, Y., Ellison, A.J., Gupta, P.K., and Allan, D.C. (2009) Viscosity of glass-

1018   forming liquids. Proceedings of the National Academy of Sciences, 106, 19780-19784.

1019   McMillan, P.F., and Kirkpatrick, R.J. (1992) Al coordination in magnesium aluminosilicate

1020   glasses. American Mineralogist, 77, 898-900.

45

1021 Murdoch, J.B., Stebbins, J.F., and Carmichael, I.S.E. (1985) High-resolution ^{29}Si NMR study of

1022   silicate and aluminosilicate glasses: the effect of network-modifying cations. American

1023   Mineralogist, 70, 332-343.

1024 Mysen, B.O. (1990) Effect of pressure, temperature and bulk composition on the structure and

1025   species distribution in depolymerized alkali aluminosilicate melts and quenched glasses.

1026   Journal of Geophysical Research, 95, 15733-15744.

1027 -. (1997) Aluminosilicate melts: structure, composition and temperature. Contributions to

1028   Mineralogy and Petrology, 127, 104-118.

1029 Mysen, B.O., and Richet, P. (2005) Silicate Glasses and Melts, Properties and Structure. 544 p.

1030   Elsevier, Amsterdam.

1031 Mysen, B.O., and Toplis, M.J. (2007) Structural behavior of Al^{3+} in peralkaline, metaluminous,

1032   and peraluminous silicate melts and glasses at ambient temperature. American Mineralogist,

1033   92, 933-946.

1034 Nasikas, N.K., Edwards, T.G., Sen, S., and Papatheodorou, G.N. (2012) Structural characteristics

1035   of novel Ca-Mg orthosilicate and suborthosilicate glasses: results from ^{29}Si and ^{17}O NMR

1036   spectroscopy. Journal of Physical Chemistry B, 116, 2696-2702.

1037 Navrotsky, A., Geisinger, K., McMillan, P., and Gibbs, G.V. (1985) The tetrahedral framework

1038   in glasses and melts: inferences from molecular orbital calculations and implications for

1039   structure, thermodynamics and physical properties. Physics and Chemistry of Minerals, 11,

1040   284-298.

1041 Neuville, D.R., Cormier, L., de Ligney, D., Roux, J., Flank, A.-M., and Lagarde, P. (2008a)

1042   Environments around Al, Si, and Ca in aluminate and aluminosilicate melts by X-ray

1043   absorption spectroscopy at high temperature. American Mineralogist, 93, 228-234.

1044   Neuville, D.R., Cormier, L., and Massiot, D. (2006) Al coordination and speciation in calcium

1045   aluminosilicate glasses: effects of composition determined by Al-27 MQ-MAS NMR and

1046   Raman spectroscopy. Chemical Geology, 229, 173-185.

1047   Neuville, D.R., Cormier, L., Montouillout, V., Florian, P., Millot, F., Rifflet, J.C., and Massiot,

1048   D. (2008b) Structure of Mg- and Mg/Ca aluminosilicate glasses: ^{27}Al NMR and Raman

1049   spectroscopy investigations. American Mineralogist, 93, 1721-1731.

1050   Neuville, D.R., and Richet, P. (1991) Viscosity and mixing in molten (Ca, Mg) pyroxenes and

1051   garnet. Geochimica et Cosmochimica Acta, 55, 1011-1019.

1052   Nichols, A.R.L., Potuzak, M., and Dingwell, D.B. (2009) Cooling rates of basaltic hyaloclastites

1053   and pillow lava glasses from the HSDP2 drill core. Geochimica et Cosmochimica Acta, 73,

1054   1052-1066.

1055   Phillips, B.L., Kirkpatrick, R.J., and Carpenter, M.A. (1992) Investigation of short-range Al,Si

1056   order in synthetic anorthite by ^{29}Si MAS NMR spectroscopy. American Mineralogist, 77, 484-

1057   495.

1058   Poe, B.T., McMillan, P.F., Rubie, D.C., Chakraborty, S., Yargar, J., and Diefenbacher, J. (1997)

1059   Silicon and oxygen self-diffusivities in silicate liquids measured to 15 gigpascals and 2800

1060   Kelvin. Science, 276, 1245-1248.

1061   Putnis, A. (1992) Introduction to Mineral Sciences. 457 p. Cambridge University Press,

1062   Cambridge.

1063   Putnis, A., Fyfe, C.A., and Gobbi, G.C. (1985) Al,Si ordering in cordierite using "magic angle

1064   spinning" NMR. Physics and Chemistry of Minerals, 12, 211-216.

47

1065   Reid, J.E., Susuki, A., Funakoshi, K.-I., Terasaki, H., Poe, B.T., Rubie, D.C., and Ohtani, E.

1066   (2003) The viscosity of $CaMgSi_2O_6$ liquid at pressures up to 13 GPa. Physics of Earth and

1067   Planetary Interiors, 139, 45-54.

1068   Richet, P. (1984) Viscosity and configurational entropy of silicate melts. Geochimica et

1069   Cosmochimica Acta, 48, 471-483.

1070   -. (2009) Residual and configurational entropy: Quantitative checks through applications of

1071   Adam-Gibbs theory to the viscosity of silicate melts. Journal of Non-Crystalline Solids, 355,

1072   628-635.

1073   Richet, P., and Bottinga, Y. (1986) Thermochemical properties of silicate glasses and liquids: a

1074   review. Reviews of Geophysics, 24, 1-25.

1075   Richet, P., and Neuville, D.R. (1992) Thermodynamics of silicate melts: configurational

1076   properties. In S.K. Saxena, Ed. Thermodynamic data, p. 132-161. Springer-Verlag, New

1077   York.

1078   Richet, P., and Ottonello, G. (2014) The Earth as a multiscale quantum-mechanical system.

1079   Comptes Rendues Geoscience, 346, 317-325.

1080   Ryerson, F.J. (1985) Oxide solution mechanisms in silicate melts: systematic variations in the

1081   activity coefficient of SiO_2. Geochimica et Cosmochimica Acta, 49, 637-650.

1082   Sen, S. (2008) Differential mobility and spatially heterogeneous dynamics of oxygen atoms in a

1083   supercooled glass-forming network liquid. Physical Review B, 78, 100201.

1084   Sen, S., and Tangeman, J. (2008) Evidence for anomalously large degree of polymerization in

1085 Mg_2SiO_4 glass and melt. American Mineralogist, 93, 946-949.

1086   Skinner, L.B., Benmore, C.J., Weber, J.K.R., Tumber, S., Lazareva, L., Neuefeind, J.,

1087   Santodonato, L., Du, J., and Parise, J.B. (2012) Structure of molten $CaSiO_3$: neutron

1088   diffraction isotope substitution with aerodynamic levitation and molecular dynamics study.

1089   Journal of Physical Chemistry B, 116, 13439-13447.

1090   Stebbins, J.F. (1995) Dynamics and structure of silicate and oxide melts: nuclear magnetic

1091   resonance studies. In J.F. Stebbins, P.F. McMillan, and D.B. Dingwell, Eds. Structure,

1092   Dynamics, and Properties of Silicate Melts, 32, p. 191-246. Mineralogical Society of

1093   America, Washington, D.C.

1094   -. (2008) Temperature effects on the network structure of oxide melts and their consequences for

1095   configurational heat capacity. Chemical Geology, 256, 80-91.

1096   Stebbins, J.F., Carmichael, I.S.E., and Moret, L.K. (1984) Heat capacities and entropies of

1097   silicate liquids and glasses. Contributions to Mineralogy and Petrology, 86, 131-148.

1098   Stebbins, J.F., Dubinsky, E.V., Kanehashi, K., and Kelsey, K.E. (2008) Temperature effects on

1099   non-bridging oxygen and aluminum coordination number in calcium aluminosilicate glasses

1100   and melts. Geochimica et Cosmochimica Acta, 72, 910-925.

1101   Stebbins, J.F., Lee, S.K., and Oglesby, J.V. (1999) Al–O–Al oxygen sites in crystalline

1102   aluminates and aluminosilicate glasses: high-resolution oxygen-17 NMR results. American

1103   Mineralogist, 84, 983-986.

1104   Stebbins, J.F., and McMillan, P. (1993) Compositional and temperature effects on five

1105   coordinated silicon in ambient pressure silicate glasses. Journal of Non-Crystalline Solids,

1106   160, 116-125.

1107   Stebbins, J.F., McMillan, P.F., and Dingwell, D.B. (1995a) Structure, Dynamics, and Properties

1108   of Silicate Melts. In P. Ribbe, Ed. Reviews in Mineralogy, 32, p. 616. Mineralogical Society

1109   of America, Washington, D.C.

49

1110   Stebbins, J.F., Sen, S., and Farnan, I. (1995b) Silicate species exchange, viscosity, and

1111   crystallization in a low-silica melt: In situ high-temperature MAS NMR spectroscopy.

1112   American Mineralogist, 80, 861-864.

1113   Stebbins, J.F., Spearing, D.R., and Farnan, I. (1989) Lack of local structural orientation in oxide

1114   glasses quenched during flow: NMR results. Journal of Non-Crystalline Solids, 110, 1-12.

1115   Stebbins, J.F., Wu, J., and Thompson, L.M. (2013) Interactions between network cation

1116   coordination and non-bridging oxygen abundance in oxide melts and glasses: insights from

1117   NMR spectroscopy. Chemical Geology, 346, 34-46.

1118   Stebbins, J.F., and Xue, X. (2014) NMR spectroscopy of inorganic Earth materials. In G.S.

1119   Henderson, D. Neuville, and R.T. Downs, Eds. Spectroscopic Methods in Mineralogy and

1120   Materials Sciences, 78, p. 605-653. Min. Soc. Am., Chantilly, VA.

1121   Stixrude, L., de Koker, N., Mookherjee, M., and Karki, B.B. (2009) Thermodynamics of silicate

1122   liquids in the deep Earth. Earth and Planetary Science Letters, 278, 226-232.

1123   Thompson, L.M., and Stebbins, J.F. (2011) Non-bridging oxygen and high-coordinated

1124   aluminum in metaluminous and peraluminous calcium and potassium aluminosilicate glasses:

1125   High-resolution ^{17}O and ^{27}Al MAS NMR results. American Mineralogist, 96, 841-853.

1126   Tinker, D., Lesher, C.E., Baxter, G.M., Uchida, T., and Wang, Y. (2004) High-pressure

1127   viscometry of polymerized silicate melts and limitations of the Eyring equation. American

1128   Mineralogist, 89, 1701-1708.

1129   Tischer, R.E. (1969) Heat of annealing in simple alkali silicate glasses. Journal of the American

1130   Ceramic Society, 52, 499-503.

1131   Toplis, M.J., and Dingwell, D.B. (2004) Shear viscosities of CaO-Al_2O_3-SiO_2 and MgO-Al_2O_3-

1132 SiO_2 liquids: Implications for the structural role of aluminum and the degree of

50

1133   polymerization of synthetic and natural aluminosilicate melts. Geochimica et Cosmochimica

1134   Acta, 68, 5169-5188.

1135   Toplis, M.J., Dingwell, D.B., Hess, K.U., and Lenci, T. (1997a) Viscosity, fragility, and

1136   configurational entropy of melts along the join SiO_2-$NaAlSiO_4$. American Mineralogist, 82,

1137   979-990.

1138   Toplis, M.J., Dingwell, D.B., and Lenci, T. (1997b) Peraluminous viscosity maxima in Na_2O -

1139 Al_2O_3 - SiO_2 liquids: the role of triclusters in tectosilicate melts. Geochimica et

1140   Cosmochimica Acta, 61, 2605-2612.

1141   Toplis, M.J., Kohn, S.C., Smith, M.E., and Poplett, I.J.F. (2000) Five coordinate aluminum in

1142   tectosilicate glasses observed by triple quantum MAS NMR. American Mineralogist, 85,

1143   1556-1560.

1144   Tossell, J.A., and Vaughn, D.J. (1992) Theoretical Geochemistry: Applications of Quantum

1145   Mechanics in the Earth and Mineral Sciences. 514 p. Oxford University Press, Oxford.

1146   Vedishcheva, N.M., Shakhmatkin, B., A., and Wright, A.C. (1998) A thermodynamic approach

1147   to the structural modeling of oxide melts and glasses: Borate and silicate systems. Glass

1148   Physics and Chemistry, 24, 308-311.

1149   Vuilleumier, R., Sator, N., and Guillot, B. (2011) Electronic distribution around oxygen atoms in

1150   silicate melts by ab initio molecular dynamics simulations. Journal of Non-Crystalline Solids,

1151   357, 2555-2561.

1152   Wilke, M., Farges, F., Partzsch, G.M., Schmidt, C., and Behrens, H. (2007) Speciation of Fe in

1153   silicate glasses and melts by in-situ XANES spectroscopy. American Mineralogist, 92, 44-56.

51

1154   Wolf, G.H., and McMillan, P.F. (1995) Pressure effects on silicate melt structure and properties.

1155   In J.F. Stebbins, P.F. McMillan, and D.B. Dingwell, Eds. Structure, Dynamics, and Properties

1156   of Silicate Melts, 32, p. 505-562. Mineralogical Society of America, Washington, D.C.

1157   Wu, J., Deubener, J., Stebbins, J.F., Grygarova, L., Behrens, H., Wondraczek, L., and Yue, Y.

1158   (2009) Structural response of a highly viscous aluminoborosilicate melt to isotropic and

1159   anisotropic compression. Journal of Chemical Physics, 131, 104504-1-10.

1160   Xue, X., Stebbins, J.F., Kanzaki, M., McMillan, P.F., and Poe, B. (1991) Pressure-induced

1161   silicon coordination and tetrahedral structural changes in alkali silicate melts up to 12 GPa:

1162   NMR, Raman, and infrared spectroscopy. American Mineralogist, 76, 8-26.

1163   Xue, X.Y. (2009) Water speciation in hydrous silicate and aluminosilicate glasses: Direct

1164   evidence from ^{29}Si-^{1}H and ^{27}Al-^{1}H double-resonance NMR. American Mineralogist, 94, 395-

1165   398.

1166   Yarger, J.L., Smith, K.H., Nieman, R.A., Diefenbacher, J., Wolf, G.H., Poe, B.T., and McMillan,

1167   P.F. (1995) Al coordination changes in high-pressure aluminosilicate liquids. Science, 270,

1168   1964-1967.

1169
1170

52

Figure Captions

1171

1172   **Figure 1.** Qualitative sketch of how a first order thermodynamic property such as molar volume,

1173   entropy, or enthalpy varies with temperature for a glass-forming liquid. The stable liquid enters

1174   the metastable ("supercooled") field on cooling below the melting point of the corresponding

1175   crystal, T_m. On further cooling, the rate at which the structure of the melt becomes more ordered

1176   slows to the point where it falls out of equilibrium, transforming to a solid glass. The properties

1177   of the glass are strongly dependent on this point of transition, T_f, which is higher for faster

1178   cooling. The colored area represents the "configurational" contribution to the property of the

1179   liquid. Note that in reality, curves are not linear, the changes in slope vary widely, and the glass

1180   transition takes place over a range in temperature, not at a single discontinuity.

1181

1182   **Figure 2.** Plot of $\log_{10}$ of viscosity (Richet, 1984) for albite (Ab, $NaAlSi_3O_8$) and diopside (Di,

1183 $CaMgSi_2O_6$) liquids, vs. inverse temperature. Straight lines (pure "Arrhenian" behavior) are

1184   shown for comparison. The glass transitions are at about 10^{12} Pa·s.

1185

1186   **Figure 3.** Sketch of a two-dimensional analog of a silica-like "crystal" vs. "glass". Here and in

1187   Figure 5, oxygen anions are shown explicitly as larger circles, cations as smaller circles. Note the

1188   relatively small number of ways that the "glass" structure is disordered relative to that of the

1189   "crystal", e.g. angles between polyhedra, ring sizes.

1190

1191   **Figure 4.** Sketch of a two-dimensional analog for adding a network-modifying oxide (M_2O) to a

1192   network liquid such as SiO_2, B_2O_3, or GeO_2. Here, network cation polyhedra are shown instead

1193   of the oxygen anions that mark each of their corners. (a) Most appropriate for silicates at low

53

1194   pressure, the added oxide forms two NBO (dark blue circles) from a bridging oxygen connecting

1195   two "tetrahedra". The nominal –1 charge on the NBO's are relatively concentrated. (b) Most

1196   appropriate for germanates or borates at low pressure (during initial modification of the

1197   network), or possibly silicates at high pressure. Here, the added oxide increases the coordination

1198   number of a network cation. Instead of forming NBO, oxygen bridges between the higher and

1199   lower coordinated network cations (light blue circles) are formed, whose partial negative charges

1200   are more dispersed than in (a). In both cases, the M cations (yellow circles) are distributed to

1201   balance the charges on the oxygens. Modified from (Stebbins et al., 2013).

1202

1203   **Figure 5.** As in Figure 3, sketch of a two-dimensional analog of a compositionally complex

1204   "chain silicate" "crystal" vs. "glass". Here there are two types of network-forming cations (Si

1205   and Al) and two types of network-modifying cations (e.g. Na and K). Some of the bridging

1206   oxygens (BO) and non-bridging oxygens (NBO) are labeled. Compared with Figure 3, there are

1207   many more ways of disordering the structure: randomization of each pair of cations; change from

1208   a single to multiple types of anionic groups; even the formation of over-coordinated Al.

1209

1210   **Figure 6**. As in Figure 4: sketch of a two-dimensional analog of a modified network liquid, but

1211   showing implications for longer-range structure. The upper panel corresponds to Figure 4a, with

1212   all "tetrahedral" network cations (triangles in 2-D) and abundant NBO. Note clustering or

1213   "channeling" of modifier cations. The lower panel corresponds to Figure 4b, with partially

1214   charged BO between lower and higher coordinated network cations. Note the much greater

1215   dispersion of the modifier ("charge balancing") cations. A transition from the upper to lower

54

1216   type of structure might take place in aluminosilicate melts with increasing pressure. Modified

1217   from (Stebbins et al., 2013).

1218

1219   **Figure 7.** The liquidus curves for cristobalite in a series of alkaline earth and alkali silicate

1220   binary phase diagrams (Ryerson, 1985), showing dramatic effect of modifier cation field strength

1221   ($Mg^{2+}>Ca^{2+}> Sr^{2+}> Ba^{2+}> Li^+> Na^{2+}> K^+$). Any series of isothermal points on the liquidi have

1222   the same silica activity, as illustrated by red dots and dashed line.

1223

1224   **Figure 8.** Activities of silica (taken here as Si_4O_8) and of alumina (Al_4O_6) calculated using the

1225   pMelts software package (Ghiorso et al., 2002) for a typical mid-ocean ridge basalt at 1600 ˚C

1226   and 1 GPa. Five compositions, each with 1 mole % of an added modifier oxide component

1227   (replacing 1% CaO), are compared to assess the effects of cation field strength in these complex

1228   compositions.

1229

1230   **Figure 9.** As in Figure 4: sketch of a two-dimensional analog of addition of alumina to a

1231   modified silicate network. Here, the concentrated negative charges on the NBO (dark blue

1232   circles) are converted to more dispersed, small negative charges (light blue circles) on BO

1233   linking Si and Al (green triangle). Modified from (Stebbins et al., 2013).

1234

1235   **Figure 10.** As in Figure 9: an expanded view of a 2-D analog structure for a glass/melt with

1236   equimolar Si and Al, to illustrate the range of possibilities from complete "aluminum avoidance"

1237   (lower panel, no Al-O-Al or Si-O-Si) to a disordered arrangement (upper panel, abundant Al-O-

1238   Al and Si-O-Si). Modified from (Henderson et al., 2006).

55

1239

1240   **Figure 11.** Schematic model of a possible mechanism of exchange between silicon and oxygen

1241   species in a liquid. Oxygens are shown as large open circles, cations as smaller filled circles. In

1242   step 1, a modifier cation moves away from an NBO (blue circle), which then forms a short-lived

1243   Si-O bond to create a ^{V}Si (black circle). If this step reverses (double arrow), there is no net

1244   diffusion, exchange, or flow. In step 2 the bonds break differently, converting the ^{V}Si back to

1245 ^{IV}Si, a former BO (green) to an NBO, and a former NBO (blue) to an NBO. If all of the

1246   unlabeled oxygens are bonded to other Si (not shown), then during this same process a Q^3 group

1247   (A) is converted to a Q^4 group and a Q^4 group (B) is converted to a Q^3 group. Cation and anion

1248   diffusion, species exchange, and a viscous flow step all have occurred. Modified from (Calas et

1249   al., 2006).

1250

1251   **Figure 12.** Hypothetical liquidus curves for two phases A with the same melting point but very

1252   different heats of melting. The intersecting liquidus for B is the same in both cases. For ΔH_m= 60

1253   kJ/mol, the eutectic (arrow) is at X_A =0.38 and 1580 K, for 3 kJ/mol, it is at X_A = 0.84 and 1000

1254   K.

1255

1256

1257

1258

1259

1260

56

- entropy or enthalpy or volume (y-axis)
- temperature (x-axis)

liquid

glass-fast cooled

glass-slow cooled

crystal

T_f

T_f

T_m
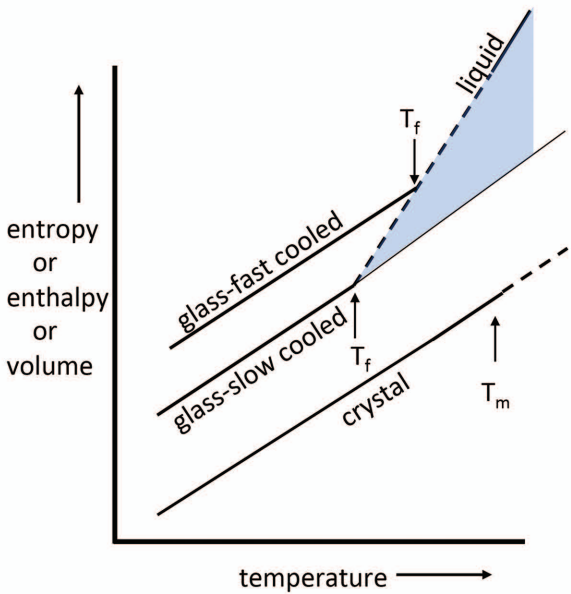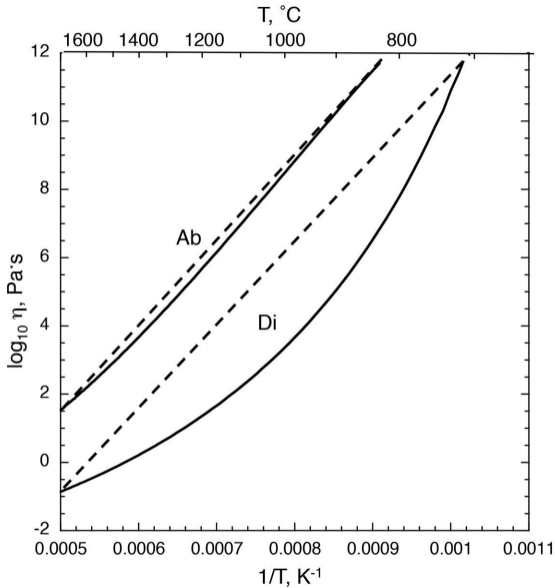
silica-like "crystal"

silica-like "glass"

○ Si　● O

a

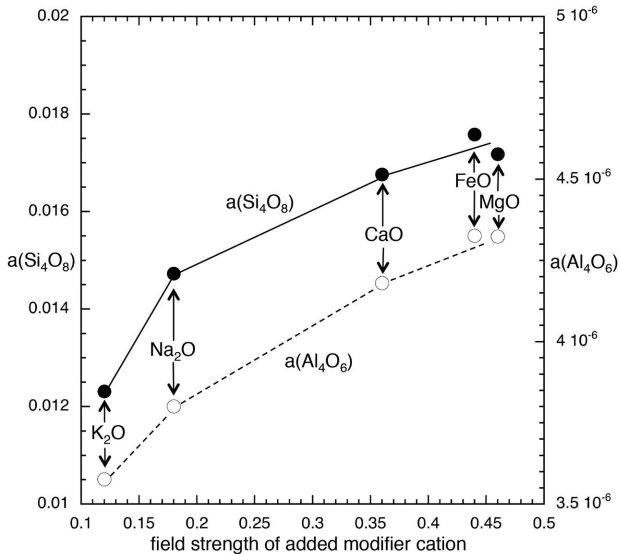+ M$_2$O →

b

+ M$_2$O →
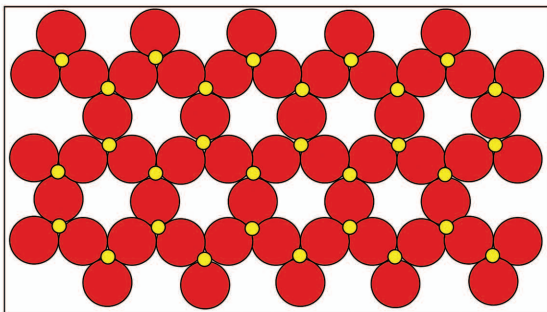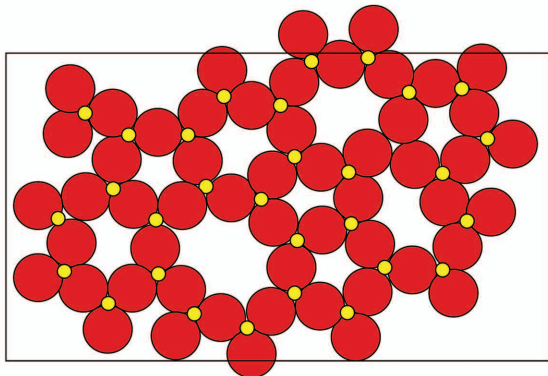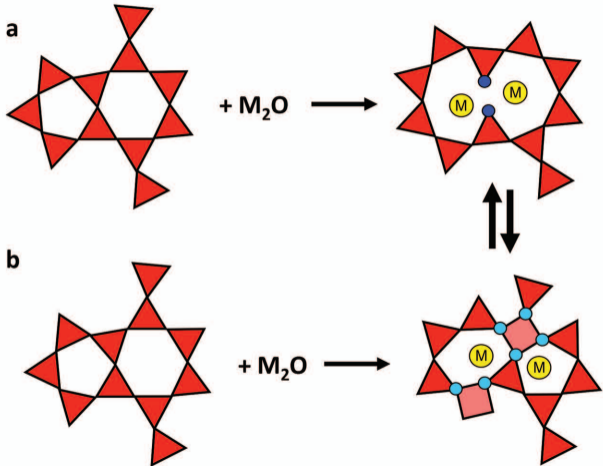
chain silicate "crystal"
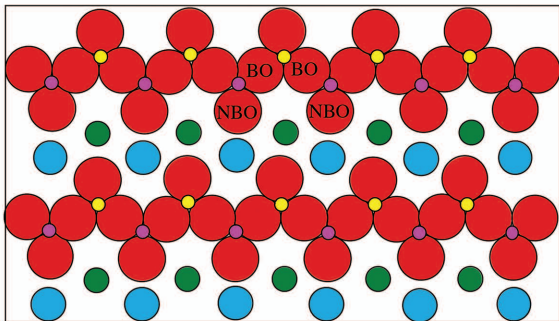
chain silicate "glass"

Si   Al   O   Na   K

Figure: Phase diagram showing temperature (T, K) versus mole fraction SiO₂ for various oxide-silica systems: MgO, CaO, SrO, BaO, Li₂O, Na₂O, K₂O. The vertical axis ranges from approximately 1200 to 2000 K, and the horizontal axis ranges from 0.5 to 1.0 mole fraction SiO_2.

$+ \tfrac{1}{2}\ Al_2O_3$
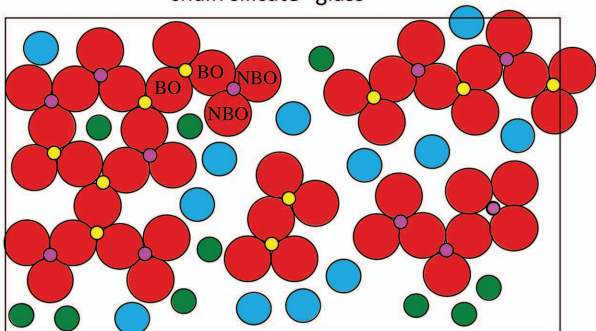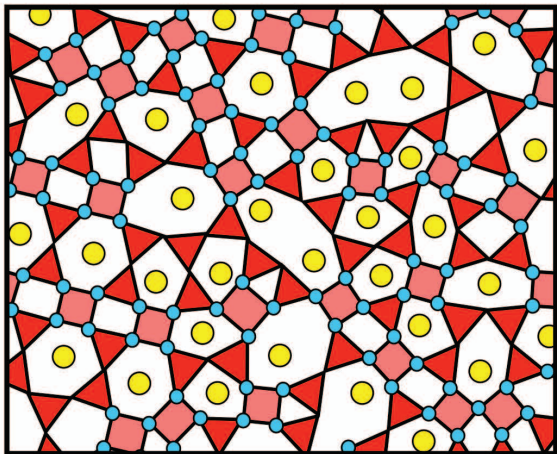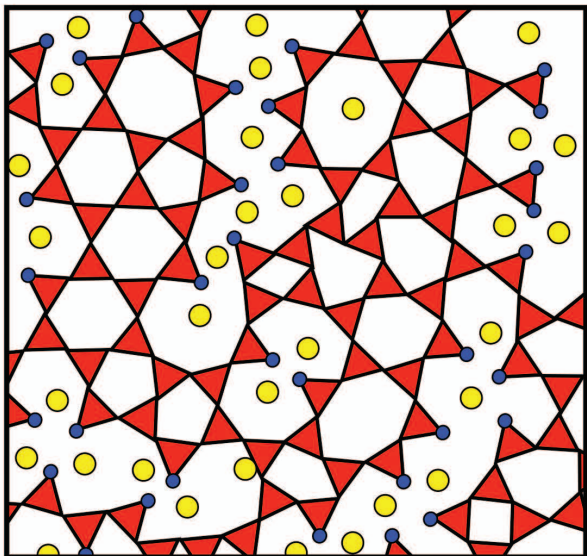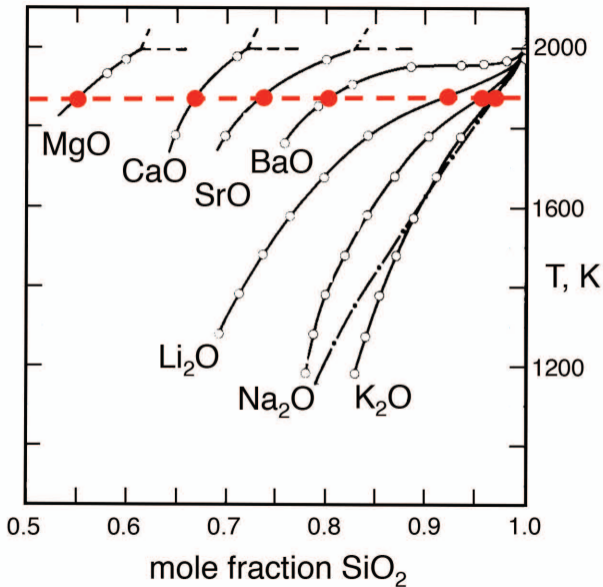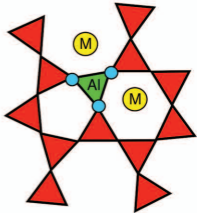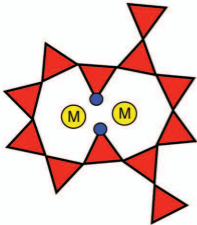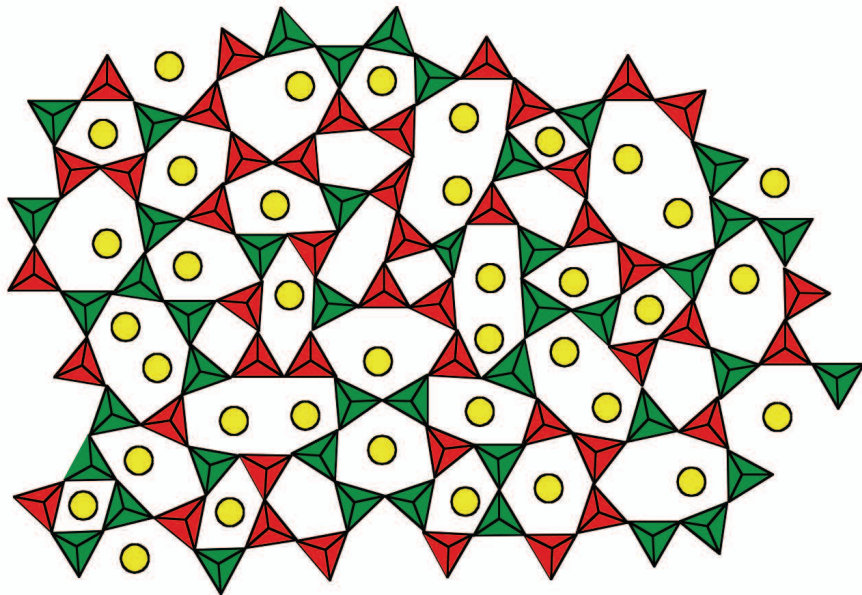
45 ▲ Si
45 ▲ Al
23 ◄► Al-O-Al

more disordered "glass": many Al-O-Al (high T?)
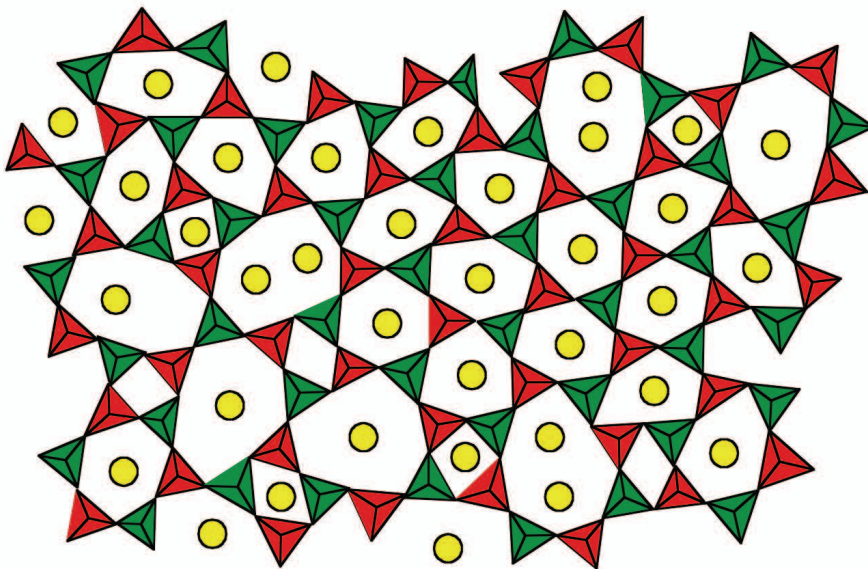
45 ▲ Si
45 ▲ Al
0 ◄► Al-O-Al

less disordered "glass": few Al-O-Al (low T?)